PB85-243160

Prediction of Selectivity for Activated Carbon Adsorption of Trace Organic (Homologue) Contaminants

Rensselaer Polytechnic Inst. Troy, NY

Prepared for

Environmental Protection Agency, Cincinnati, OH

Jul 85

PB85-243160

EPA/600/2-85/093
July 1985

PREDICTION OF SELECTIVITY FOR ACTIVATED CARBON ADSORPTION OF TRACE ORGANIC (HOMOLOGUE) CONTAMINANTS

by

Georges Belfort, Cheng-Sheng Lee, Roger J. Weigand, and Diane M. Neuhaus
Rensselaer Polytechnic Institute
Troy, New York 12180

Grant No. CR-809686-01-0

Project Officer

Richard A. Dobbs
Wastewater Research Division
Water Engineering Research Laboratory
Cincinnati, Ohio 45268

WATER ENGINEERING RESEARCH LABORATORY
OFFICE OF RESEARCH AND DEVELOPMENT
U.S. ENVIRONMENTAL PROTECTION AGENCY
CINCINNATI, OHIO 45268

REPRODUCED BY
NATIONAL TECHNICAL
INFORMATION SERVICE
U.S. DEPARTMENT OF COMMERCE
SPRINGFIELD, VA. 22161

TECHNICAL REPORT DATA (Please read Instructions on the reverse before completing)		
1. REPORT NO. EPA/600/2-85/093	2.	3. RECIPIENT'S ACCESSION NO. PB85 243160/AS
4. TITLE AND SUBTITLE Prediction of Selectivity for Activated Carbon Adsorption of Trace Organic (Homologue) Contaminants		5. REPORT DATE July 1985 6. PERFORMING ORGANIZATION CODE
7. AUTHOR(S) G. Belfort, C. Lee, R. Weigand and D. Neuhaus		8. PERFORMING ORGANIZATION REPORT NO.
9. PERFORMING ORGANIZATION NAME AND ADDRESS Rensselaer Polytechnic Institute Troy, New York 12181		10. PROGRAM ELEMENT NO. 11. CONTRACT/GRANT NO. CR-809686-01
12. SPONSORING AGENCY NAME AND ADDRESS Water Engineering Research Laboratory -- Cin., OH Office of Research and Development U.S. Environmental Protection Agency Cincinnati, Ohio 45268		13. TYPE OF REPORT AND PERIOD COVERED Final 9-28 to 12-84 14. SPONSORING AGENCY CODE EPA/600/14
15. SUPPLEMENTARY NOTES Project Officer: Richard A. Dobbs, (513) 684-7649		

16. ABSTRACT

Preferential adsorption of organic compounds onto activated carbon from dilute aqueous solutions was studied to develop a comprehensive theoretical basis for predicting adsorption of multicomponent solutes. We investigated in this research program a comparison of different carbons, the adsorption behavior with variable aqueous solution properties, and the difference between gas and liquid phase adsorption. The overall objective was to develop and test the comprehensive solvophobic theory.

Experimental adsorption isotherms of a series of alcohols on five different carbons were measured and compared. Isotherms were run for 4-n-propyl phenol at various concentrations of ammonium sulfate salt and methanol as the additives to increase or decrease surface tension of solution, respectively. Also, isotherms for three linear carboxylic acids were measured at different pHs to determine the effect on adsorption.

An experimental-glass vacuum system has been designed and built to measure adsorption isotherms in the gas phase. A comparison of measurements of adsorption isotherms for four alcohols in the aqueous and gas phases was conducted and confirmed the theoretical model.

17. KEY WORDS AND DOCUMENT ANALYSIS		
a. DESCRIPTORS	b. IDENTIFIERS/OPEN ENDED TERMS	c. COSATI Field/Group
Adsorption Organic compounds	Activated carbon treatment	07
18. DISTRIBUTION STATEMENT RELEASE TO PUBLIC	19. SECURITY CLASS (This Report) UNCLASSIFIED	21. NO. OF PAGES 82
	20. SECURITY CLASS (This page) UNCLASSIFIED	22. PRICE

EPA Form 2220-1 (9-73)

DISCLAIMER

The information in this document has been funded wholly or in part by the United States Environmental Protection Agency under assistance agreement number CR809686-01-0 to Rensselaer Polytechnic Institute. It has been subject to the Agency's peer and administrative review, and it has been approved for publication as an EPA document. Mention of trade names or commercial products does not constitute endorsement or recommendation for use.

FOREWORD

The U.S. Environmental Protection Agency is charged by Congress with protecting the Nation's land, air, and water systems. Under a mandate of national environmental laws, the agency strives to formulate and implement actions leading to a compatible balance between human activities and the ability of natural systems to support and nurture life. The Clean Water Act, the Safe Drinking Water Act, and the Toxics Substances Control Act are three of the major congressional laws that provide the framework for restoring and maintaining the integrity of our Nation's water, for preserving and enhancing the water we drink, and for protecting the environment from toxic substances. These laws direct the EPA to perform research to define our environmental problems, measure the impacts, and search for solutions.

The Water Engineering Research Laboratory is that component of EPA's Research and Development program concerned with preventing, treating, and managing municipal and industrial wastewater discharges; establishing practices to control and remove contaminants from drinking water and to prevent its deterioration during storage and distribution; and assessing the nature and controllability of releases of toxic substances to the air, water, and land from manufacturing proesses and subsequent product uses. This publication is one of the products of that research and provides a vital communication link between the researcher and the user community.

Although activated carbon adsorption has been widely used for color, taste, and odor removal in the water industry, only recently has it been considered serioiusly for the removal of specific dissolvent organic compounds from water supplies. The work reported here includes a comparison of different carbons, the adsorption behavior with variable aqueous solution properties, and the differences between gas and liquid phase adsorption. The overall objective was to develop and test the comprehensive solvophobic theory.

Francis T. Mayo, Director
Water Engineering Research Laboratory

ABSTRACT

Preferential adsorption of organic compounds onto activated carbon from dilute aqueous solutions was studied to develop a comprehensive theoretical basis for predicting adsorption of multicomponent solutes. The investigation includes a comparison of different carbons, the adsorption behavior with variable aqueous solution properties, and the differences between gas and liquid phase adsorption. The overall objective was to develop and test the comprehensive solvophobic theory.

Experimental adsorption isotherms of a series of alcohols on five different carbons were measured and compared. Isotherms were run for 4-n-propyl phenol at various concentrations of ammonium sulfate salt and methanol as the additives to increase or decrease surface tension of solution, respectively. Also, isotherms for three linear carboxylic acids were measured at different pH's to determine the effect on adsorption.

An experimental-glass vacuum system has been designed and built to measure adsorption isotherms in the gas phase. Measurements of adsorption isotherms for four alcohols were conducted in the aqueous and gas phases and confirmed the theoretical model.

The development of predictive techniques for multi-component adsorption based on the use of an equation of state were compared with the Ideal Adsorbed Solution (IAS) theory using competitive phenol adsorption data.

This report was submitted in fulfillment of Grant No. CR-809686-01-0 by Rensselaer Polytechnic Institute under sponsorship of the U.S. Environmental Protection Agency. This report covers the period 9/13/82 to 9/12/84, and the work was completed on 12/12/84.

CONTENTS

Foreword iii
Abstract iv
Figures vi
Tables viii
List of Symbols ix
Acknowledgments xii

1. Introduction 1
   Background 1
   Objectives 1
2. Conclusions 3
3. Recommendations 5
4. Experimental 6
   Characterization of sorbents 6
   Absorbates 6
   Pretreatment of sorbents 6
   Variation of solution property 6
   Adsorption isotherm procedure 6
   Data analysis 11
   Statistical methods 12
5. Theoretical 14
   General solvophobic approach 14
   Thermodynamic of gas phase adsorption 21
   Surface tension and aqueous adsorption 25
   Multi-component adsorption 27
6. Results and Discussion 32
   Comparison between different carbons 32
   The differences between gas and liquid phase adsorption . . 32
   General solvophobic approach 38
   Surface tension effect on adsorption 47
   pH effect on adsorption 53
   Multi-component adsorption 53

References 67

FIGURES

Number		Page
1.	Experimental adsorption apparatus in liquid phase	9
2.	Experimental adsorption apparatus in gas phase	10
3.	Association adsorption reaction	15
4.	Adsorbability ($\ln Q°_b$) versus MW for linear alcohols	33
5.	Adsorbability ($\ln Q°_b$) versus cavity surface area for linear alcohols	34
6.	Langmuir model parameters versus molecular weight for the adsorption of linear alcohols from gas and liquid phases	37
7.	$\ln Q°_b$ versus solute molecular weight for linear alcohols and water in solution	39
8.	$\Delta G^{net}_{solvent\ effect}/RT$ and $\Delta G^{assoc}_{gas}/RT$ versus carbon number for the aliphatic alcohols	43
9.	$\Delta G^{assoc}_{gas}/RT$ and $\Delta G^{assoc}_{solvent}/RT$ versus carbon number for the aliphatic alcohols	45
10.	$\ln Q°_b$ and $\ln bp_s$ as a function of $\Delta G^{assoc}_{solvent}$ and ΔG^{assoc}_{gas} respectively	46
11.	Correlation coefficients and confidence intervals for the correlation of $\ln Q°_b$ with solute parameters for the alcohols	48
12.	Adsorption isotherms for 4-n-propylphenol in solvents of varying salt concentration (0~1.143 M)	50
13.	Adsorption isotherms for 4-n-propylphenol in solvents of varying salt concentration (1.143~1.714 M)	51
14.	Adsorption capacity and adsorbability versus salt concentration and solvent surface tension for 4-n-propylphenol	52
15.	Adsorption isotherms for 4-n-propylphenol in solvents of varying volume percent of methanol	54
16.	$Q°$ and $\ln Q°_b$ versus volume percent methanol for 4-n-propylphenol	55

17. $\ln Q^{\circ}_b$ versus solvent surface tension for 4-n-propylphenol 56

18. Adsorbability versus molecular weight for carboxylic acids at different pHs. 57

19. Adsorbability versus total cavity surface area for carboxylic acids at different pH's 58

20. Single-solute adsorption isotherm for alkyl phenols 59

21. Surface-tension isotherm for alkyl phenols. 62

22. The analog compressibility factor as a function of adsorbed alkyl phenols 63

23. The iterative scheme for testing theory 64

24. Adsorption from aqueous multi-solute system (4-n-methylphenol and 4-n-propylphenol) at low initial concentrations 65

25. Adsorption from aqueous multi-solute system (4-n-methylphenol and 4-n-propylphenol) at higher initial concentrations 66

TABLES

Number		Page
1.	Properties of absorbents.	7
2.	Correlation coefficient r for Langmuir adsorption parameters versus molecular weight and total surface area for the alkyl alcohols on five different carbons.	35
3.	Langmuir adsorption parameters for the alkyl alcohols on five different carbons	36
4.	Calculated values for r_s^d for adsorption of linear alcohols onto porous activated carbon.	40
5.	Physical properties of the aliphatic alcohols	41
6.	Physical properties and solvophobic contributions for the alcohols.	42
7.	Adsorption isotherm measurements fitted to the Langmuir model for 4-n-propylphenol in solvents of varying surface tension . . .	49
8.	Characteristics constants for alkyl-phenols	60

LIST OF SYMBOLS

A	Specific surface area of adsorbent, m^2/g
$\tilde{a}_i$	Coefficient of thermal expansion
a_i	Molar area occupied by adsorbate surface layer, $cm^2/mole$
b	Langmuir isotherm parameter, $torr^{-1}$ or $\ell/mmole$
c	Adsorbate concentration in solution, mmole/g
D	Electrostatic variable, Eq.(22)
G	Gibbs free energy, kcal/mole
I	Ionization potential, eV
K	Reaction equilibrium constant
l_i	Kihara Parameter
MW	Molecular weight
N	Reciprocal of molecular volume, $Å^{-3}$
N_a	Avogadro's number
n_D	Index of refraction
P	Electrostatic variable, Eq.(22)
p	Pressure, torr
p_s	Saturation pressure, torr
$[P]$	Parachor
$Q°$	Langmuir isotherm parameter, mmole/g
q	Adsorbent loading, mmole/g
R	Universal gas constant
R_i	Molecular diameter, Å
T	Temperature, K
TSA	Adsorbate molecular area, $Å^2$
V	Molar volume, $cm^3/mole$

Greek Symbols

α	Parameter in confidence interval
α_i	Polarizability, Å^3
γ	Interfacial free energy, ergs/cm^2
κ^e	Energy correction for curved surface
κ^s	Entropy correction for curved surface
λ	Complex/solute volume ratio
σ	London parameter
π	Spreading pressure, ergs/cm^2
μ	Dipole moment, Debyes
ν	Molecular volume, Å^3
ρ	Density, g/cm^3

Superscripts

assoc	Association reaction, Eqn. 1
net	Product minus reactants
d	London dispersion contributions
$-$	Average

Subscripts

cav	Cavity interaction
C	Carbon (adsorbent)
es	Electrostatic interaction
gas	Gas phase reaction
i	ith solute
ℓ	Liquid
s	Solid

sg	Solid/gas interface
sℓ	Solid/liquid interface
S_i	Solute
S_iC	Carbon-solute complex
solvent	Solvent phase reaction
vdw	van der Waals' interaction
RPI	Rensselaer Polytechnic Institute

ACKNOWLEDGMENTS

The authors thank Mr. van der Gouw for building the glass vacuum system, Thomas Neubauer for keeping the system working and doing the GC/MS analysis, Gordon Altshuler and Irving Packard for helping with the computer programs, and Dr. Cynthia Hirtzel for suggesting methods of statistical analyses. The activated carbon used in this study was supplied by D.G. Chalmers, The Calgon Corp., Pittsburg.

The authors also appreciated the laboratory assistance of Mark Gessner, Tom Giroux and Carol Paradis.

SECTION 1

INTRODUCTION

BACKGROUND

Although activated carbon (AC) adsorption has been used widely for odor and color removal in the water industry, only recently has it been seriously considered for removal of dissolved organics from water supplies (1). This recent interest is caused primarily by the growing concern for potential carcinogenic, mutagenic, and teratogenic compounds found in drinking waters (2,3).

With respect to solid-liquid adsorption, a major limitation of the various equilibrium theories of adsorption (besides the adaption of the partial solubility parameter theory by McGuire and Suffet) is that they were originally derived from gas and vapor phase adsorption, and thereby a priori ignored the presence of the solvent during solute adsorption. These include the most popular and widely used approaches, which are based on Gibbs' adsorption isotherm (4,5,6), and the compressed film theory of Polanyi (7). Belfort (8) has shown recently that the Polanyi and the IAS theory based on Gibb's adsorption isotherm have similar thermodynamic structure.

Recent attempts to include the solvent effect in aqueous phase adsorption include a semi-empirical approach based on partial solubility parameters called the net adsorption energy approach (9). Unfortunately, the arbitrary choice of the relative values for the acid and base hydrogen bonding solubility parameters is without theoretical justification and renders this approach somewhat capricious (9).

During the past several years, a concerted effort has been made in RPI's laboratory to understand the role of the solvent during liquid-solid approach (10,11,12). A theoretical basis for predicting a priori the preferential adsorption of organic compounds in the same homologous series on activated carbon from dilute aqueous solution has been derived and used with confidence to rank-order single solute isomers (alcohols, ketones, and phenols) with respect to their adsorption potential (11,12). Clearly, the ability to predict the effects of structure on the adsorption of organic molecules between different homologous series from dilute aqueous solutions could be of great value in the design and operation of large scale commercial plants.

OBJECTIVES

The objectives of this study were as follows:

1. A comparison of different activated carbons using a well characterized model homologous series (linear alcohols),

2. An evaluation of the effects of surface tension on adsorption by changing the concentration of ammonium sulfate salt and methanol,

3. An evaluation of the effects of pH on carboxylic acids adsorption,

4. The further development of the comprehensive solvophobic theory by estimating the value of the gas phase term. This involved measuring the gas phase adsorption of the same homologous series as that measured from the liquid phase, and

5. The development of predictive techniques based on the use of an equation of state for multicomponent adsorption from mixtures.

Adsorption capacity for specific single organic solutes of a homologous series is thought to be a direct function of: (1) the adsorbate properties, (2) the solution conditions, and (3) the nature of the adsorbent. Little quantitative information is known about the surface characteristics of carbon, the solution properties, and their influence on organic adsorptive selectivity. The general thrust of the study is to extend both the theoretical formulations and experimental data base with the objective of developing a comprehensive theoretical basis including the important factors on adsorption for predicting a priori the preferential adsorption of organic compounds on activated carbon from aqueous solution.

SECTION 2

CONCLUSIONS

The work reported here involves the development of a comprehensive theoretical basis for predicting the preferential adsorption of organic compounds onto activated carbon from dilute aqueous solution. A detailed analysis including the characteristics of adsorbents, the effect of solution properties, and the differences between gas and liquid phase adsorption yields an insight into the adsorption process. This, together with the solvophobic theory, provides a quantitative description of all the important factors on adsorption.

The solvophobic theory is tested using single-solute aqueous-phase adsorption isotherms of a series of alcohols on different carbons. Correlations with adsorption capacity for the simplified solvophobic theory parameter, absorbate molecular area (TSA), are all in good agreement with theory for all five different carbons. Despite the steric hindrance (pore size and pore size distribution), both the adsorption capacity and adsorbability show no apparent correlation with surface area of adsorbents. It seems that the surface energy of the adsorbent has an important effect on the adsorption process.

Adsorbability of 4-n-propylphenol increases linearly with increasing ammonium sulfate concentration (or surface tension) up to a critical concentration of about 1.143 M. At higher concentrations the adsorbability decreases, deviating from the theory. This result is explained by incomplete adsorption and precipitation arguments. Adsorbability decreases linearly with the volume percent of methanol present in the solvent. Solvent surface tension is not a linear function of methanol concentration, so adsorbability does not correlate linearly with surface tension. The variability of the parameter κ^e in the solvophobic theory is invoked to explain this result; however, competitive effects resulting from the methanol may also be present.

The adsorption capacity of carboxylic acids exhibit a definite increase as the pH is decreased from 7.00 to 4.75. This can be explained by noting that a low pH increases the relative amount of a-polar undissociated carboxylic form. The solvophobic theory is also tested using carboxylic acids at different pH. Correlations with adsorption capacity for the simplified solvophobic theory parameter, TSA, is only in good agreement with theory at pH 7.00. Surface interactions at low pH probably complicate matters.

The solvophobic theory successfully correlates both gas and liquid phase adsorbabilities ($\ln bp_s$ and $\ln Q°b$ respectively) for the alcohols. It also predicts the reversal in order of preferential adsorption with molecular weight because of the presence of liquid water. The complete and simplified $c\phi$ theory is also used to correlate adsorbability from solution for homologous series of alcohols, ketones and phenols. In all three cases, the simplified theory is found to be sufficient, and molecular weight can be ruled out as a correlating parameter for adsorbability.

The adsorption isotherms of dilute aqueous solutions containing 4-n - methylphenol and 4-n-propylphenol are measured over a concentration range of 0.1 - 0.001 mole/ℓ on activated carbon at 20°C. The experimental results agree better with equilibrium predictions based on a two-dimensional adsorbed phase represented by a van der Waals' equation of state than by an ideal adsorbed solution theory, especially for the weak adsorbate. It appears that the ideal adsorbed solution theory is reliable for multicomponent systems where solute adsorption loading is low. When solute adsorption loading is high, the non-ideality of mixing in the adsorbed phase is related to constants in the two-dimensional equation of state to allow for solute-solute interactions on the surface.

SECTION 3

RECOMMENDATIONS

Myers and Sircar (13) have recently reported an asymptotic principle of correspondence for physical adsorption equilibria on heterogeneous and microporous surfaces. They propose a dimensionless group [mRT ln $(p/p_o)/\Delta G$] as a universal function of θ (fractional filling of micropores); where m is the saturation capacity and ΔG is the free energy of immersion of the adsorbent in the pure liquid sorbate. It may be possible to predict ΔG for homologous series of adsorbate, using the solvophobic theory (O. Sinanoglu, private communication). In addition to the free energy of immersion approach of Myers and Sircar (13), gas phase adsorption data have been used in RPI's laboratory to estimate the dispersion contribution of the surface free energy of the adsorbent. Combining the statistical mechanical theories of adsorption from solution by Everett (14) with the relationship between interfacial tension and tensions (15), it can be shown that both the total surface area of the solute and the surface free energy of the adsorbent are important factors for rank-ordering adsorption potential. A linear relationship between total surface area of solute and Gibbs free energy change of adsorption from solution has been demonstrated by the solvophobic theory (10,11,12). Thus, a comprehensive experimental data-base of surface free energy for adsorption from the gas phase (16) and its influence on organic adsorption selectivity will provide insight into the adsorption process. This, together with the solvophobic theory, will provide a quantitative description of the role of the solvent and the effects of structural modifications of organic molecules on adsorption.

Minka and Myers (17) have used a surface excess thermodynamic approach for multi-component adsorption. The objective of their work was to predict multi-component adsorption in terms of the binary solution adsorption parameters from the Redlich-Kister equation for estimating activity coefficients of each species in the adsorbed phase. They presented data on adsorption from hydrocarbon mixtures of benzene + cyclohexane + ethyl acetate by an active carbon; the adsorption in tertiary mixtures calculated from binary data is claimed to be within the experimental uncertainty of the data.

The approach we recommend is based on the total amount adsorbed on the surface rather than the surface excess. This can be estimated with a knowledge of the single solute adsorbabilities from aqueous (10,11,12) and gas phase at saturation (16). Also, an alternative thermodynamic approach uses Wilson (18) and UNIQUAC (19) for estimating the activity coefficients of the adsorbed components with the ultimate aim of predicting adsorption behavior from multi-component aqueous adsorption.

SECTION 4

EXPERIMENTAL

CHARACTERIZATION OF SORBENTS

The sorbent properties are presented in Table 1. The nitrogen adsorption characterization studies were performed in a surface-area pore-volume analyzer (Model 2100E, Micrometrics Inst. Corp., GA).

ADSORBATES

All the chemicals used in this study were of the highest grade (>99% purity). The alkyl phenols were obtained from Supelco (PA) and the alcohols from the Aldrich Co. (Wisc.). Stock solutions of the individual alcohols or phenols were made up with standard 0.01 m phosphate buffer (pH 7.00) and stored in amber glass or aluminum covered bottles. Carboxylic acids were obtained from Aldrich Co. (Wisc.) and prepared in phosphate buffer solutions of pH 4.75 and 7.00.

PRETREATMENT OF THE SORBENTS

The entire samples were washed four times with deionized bacteria free water to remove extraneous solutes such as salts or colloids. The samples were magnetically stirred in 9-ℓ glass carboys and the wastewater decanted and replaced every 24 hours. After the last washing, the water was decanted and the carbon samples placed in a vacuum oven (Isotemp. NO. 281, Fisher Scientific, NY) at 100°C and 25 mmHg vacuum for about 5 days until dry. The oven temperature was then increased to 120°C to remove extraneous volatile organics until constant weight was attained. The sample were then stored over CaO in a desiccator.

About 48 hours before use, the carbon was placed into autoclaved deionized water and agitated with a magnetic stirrer to allow complete water adsorption.

VARIATION OF SOLUTION PROPERTY

Methanol was purchased from MCB Manufacturing Chemists Inc. (NJ) and was certified 99.9% pure. The ammonium sulfate was purchased from Fisher Scientific (NJ) and was certified 100% pure. Stock solutions of ammonium sulfate were prepared at various concentrations between 0.5 and 3.0 M.

ADSORPTION ISOTHERM PROCEDURE

For the liquid phase, several innovations have been introduced into the adsorption isotherm procedures in an attempt to improve reproducibility and accuracy and reduce solute losses. The temperature was kept constant at 20 ± 0.5°C during this study.

TABLE 1

Properties of Adsorbents

Property/Trade Name	Filtrasorb 400	SA4	SA Plus	W20	D10
Apparent density (g/cm^3)	0.478	0.476	0.345	0.562	0.565
Pore volume (cm^3/g)	0.95	0.46	0.70	0.31	0.31
Surface area (m^2/g)	1031	690[a]	930[a]	540[a]	530[a]
Iodine adsorption (mg/g)	1200	715	1040	590	580
Manufacturer	Calgon Corp. Pittsburgh, PA	Norit Research Lab. Amersfoort, The Netherlands	Norit Research Lab. Amersfoort, The Netherlands	Norit Research Lab. Amserfoort, The Netherlands	Norit Research Lab. Amserfoot, The Netherlands

[a] estimated by manufacturers

To minimize extraneous solute-loss and maximize solute/sorbent contact the following steps and precautions were taken:

a) Adsorption was conducted in completely filled and capped 38 ml stainless steel centrifuge tubes (Part No. 301112, Beckman, CA). Thus there was no head-space for possible solute loss to the gas phase, and the solutions were only exposed to stainless steel surfaces for both minimum adsorption loss and to reduce the possibility of introducing extraneous organics.

b) The completely filled tubes were rotated end-over-end 360° at 2 rpm in a constant-temperature bath (20 ± 0.5°C;see Fig. 1). This allowed the carbon to fall the length of the tube twice per rotation resulting in good mixing and increased effective external film mass transfer coefficient. The time to reach pseudo equilibrium (i.e., >95% of the 14th day saturation value, Q°) varied from two to several hours depending on the kinetics of the particular solute and rotation rate. The mixing period employed in this study was 24 hours.

c) Once pseudo equilibriuim was attained, the tubes were placed directly into an ultracentrifuge (Model L8-55, Beckman, CA) and the carbon was spundown at 20,000 rpm for 20 min.

d) The residual phenol concentrations were measured from aliquots of the supernatant by UV-spectroscopy (Model 552, Perkin Elmer, NJ). An automatic sipping device run by a positive displacement pump was used to measure the solution solute concentration directly from the centrifuge tube. The maximum adsorbance wavelength was determined for each alkyl phenol and a corresponding calibration curve of adsorbance versus concentration was prepared.

Total organic carbon analysis (TOC) was used for measuring residual alcohol or carboxylic acid concentrations. A calibration curve was prepared from standard stock solutions before each analysis. A detectable limit of 0.5 ppm was achieved.

To identify individual solutes from a mixture of alkyl phenols, the solutes were extracted with methylene chloride, separated in the gas chromatograph (Signa 4, Perkin Elmer, NJ) and quantified in a mass spectrometer (Model 1020, Finnigan, CA).

One complication was encountered when ammonium sulfate was present. It has an adsorbance of its own, independent of the phenol concentration, but dependent on the salt concentration. Since the salt concentration was constant in each tube for a given isotherm, a constant adsorbance was measured and subtracted from the total adsorbance of each sample, thereby correcting for the presence of ammonium sulfate salt. This problem was not encountered when methanol was present since methanol is not a UV-adsorber.

The vacuum system used in the gas phase adsorption/desorption experiments is shown in Figure 2. This system, made of glass, was designed to minimize contamination from vacuum grease on the adsorption side of the cold trap.

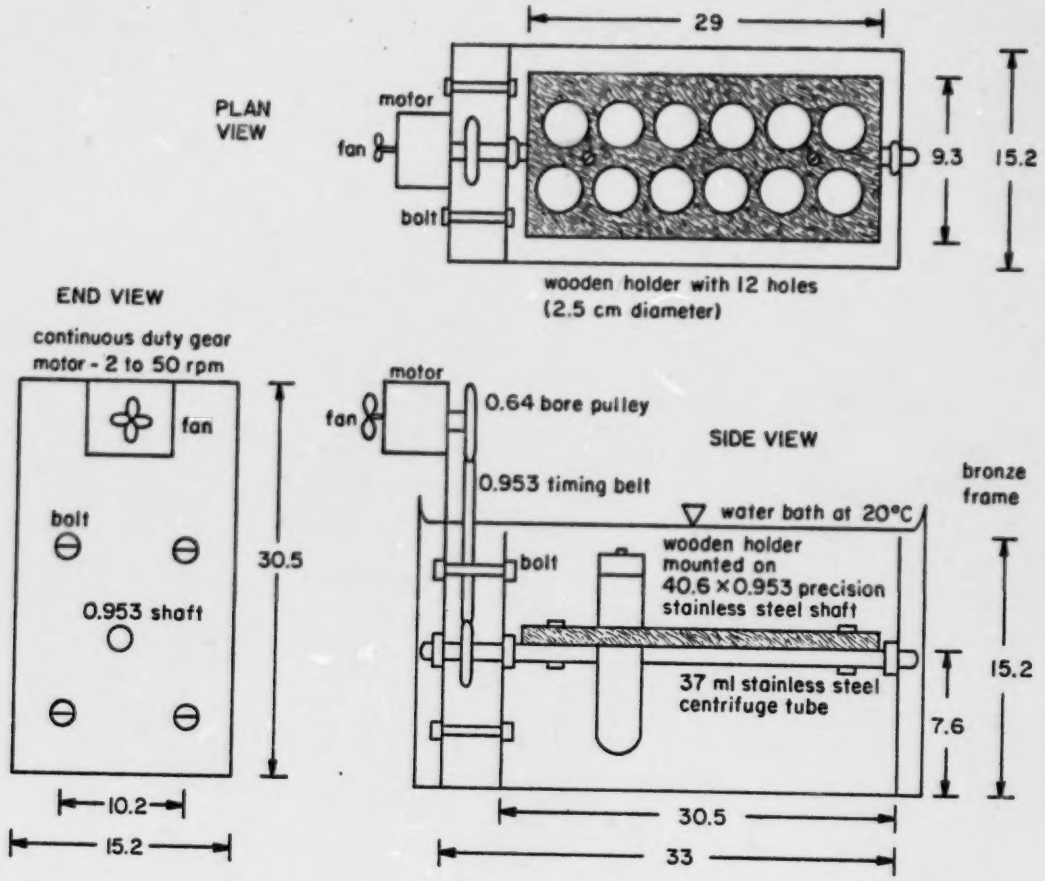

Figure 1. Experimental adsorption apparatus in liquid phase

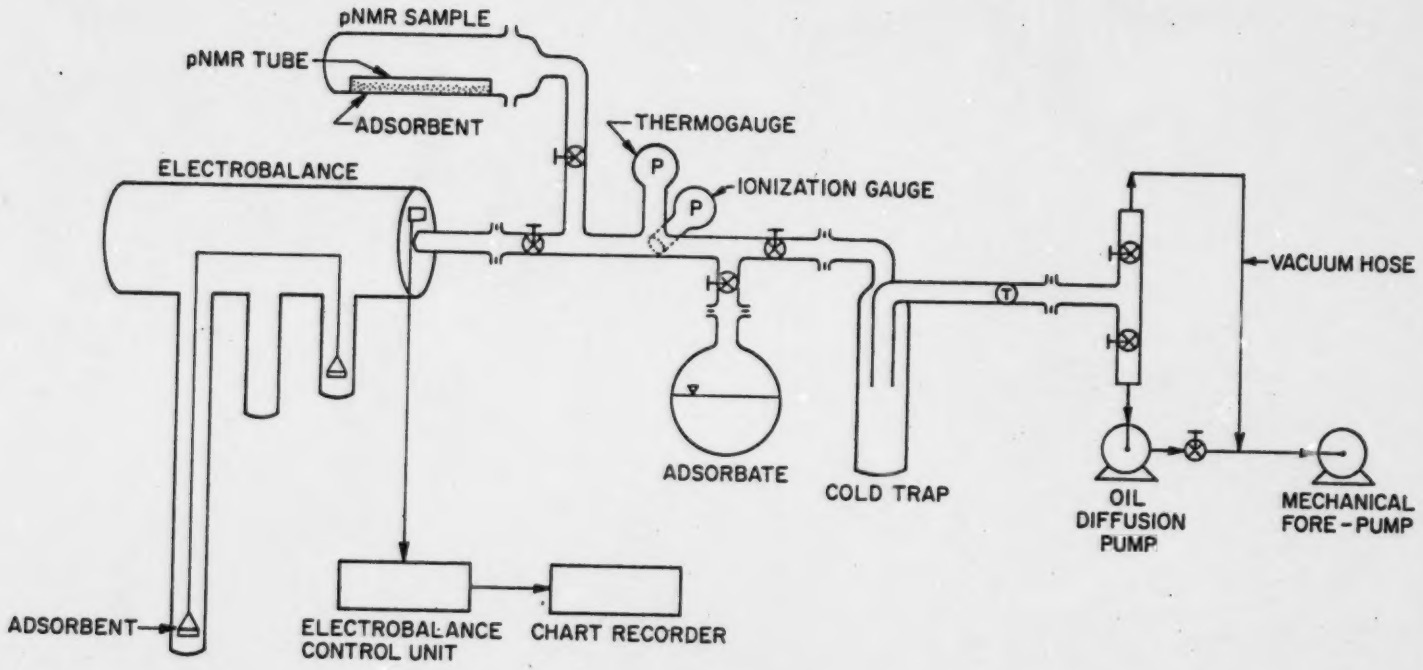

Figure 2. Experimental adsorption apparatus in gas phase

Stopcocks 1 through 4 were high-vacuum, teflon-sealed, semi-needle valves with 5 mm openings (Ace Glass, New Jersey). The ionization gauge was attached directly to the Apiezon wax. All of the glass joints were sealed using screw clamps and Buna-N o-rings with a minimal amount of silicone vacuum grease.

On the pump side of the cold trap, a three-way glass valve (stopcock 5) was used both to evacuate and to vent the adsorption system. Valves 6 through 8 were teflon-sealed Rotaflo stopcocks (Fisher Scientific Corp., New York) which were used during the operation of the pumping system.

The amount of alcohol adsorbed onto the 55 mg activated carbon hangdown sample shown in Figure 1 was measured directly using a Cahn 2000 Recording Electrobalance (Cahn Instruments, CA).

The alcohol in the adsorbate flask was frozen and evacuated to at least 10^{-3} torr. After closing stopcock 3, the adsorbate was then permitted to thaw leaving only the liquid alcohol and its vapor in the flask.

The carbon samples were outgassed in situ for up to 24 hours by heating to 200°C at 10^{-3} torr until the recorded mass of the hangdown sample remained constant. Small amounts of alcohol vapor were admitted to the system during outgassing to "flush out" any tightly adsorbed molecules from the carbon.

Blank runs without sorbent were performed with each alcohol to determine the possible effect of buoyancy on the mass readings. The procedure used was identical to that used during actual isotherm measurements.

After outgassing was completed, the first small dose of alcohol was admitted and constant temperature baths (20°C) were installed around the carbon samples. Equilibrium between the adsorbent samples and the surrounding vapor was considered to have been reached when the mass readings remained constant within 0.1 mg for two hours, representing a change of less than 0.1% of the total sample mass per hour. This usually took between 24 and 36 hours which was about the same time needed to reach equilibrium for the aqueous system (5). The only exception was for 1-heptanol where the mass continued to rise for a much longer period indicating that equilibrium was probably not reached with this compound. The instrumental limit of error is estimated to be 4%.

The final mass of the sample and the final pressure in the system were used to represent one point on the isotherm. Successive points were determined by admitting small doses of alcohol and recording the equilibrium mass and pressure readings until the final system pressure was nearly to the vapor pressure of the pure alcohol. The desorption isotherm was then determined in a similar, stepwise fashion by heating and evacuating the carbon samples. Mass and pressure readings were recorded at equilibrium.

Data Analysis

Computer programs were written to analyse the data with both the Langmuir and B.E.T. models. Only the Langmuir model was used in this study since the

fit of the data was satisfactory and a more complicated 3-parameter model such as the B.E.T. was not necessary. Other models, such as the Freundlich, were ruled out because of their thermodynamic inconsistancy at infinite dilution. The linearized form of the Langmuir model for aqueous phase and gas phase adsorption are given

$$\frac{1}{q} = \frac{1}{Q^\circ} + \frac{1}{Q^\circ b}\ \frac{1}{C} \tag{1}$$

and

$$\frac{p/P_s}{q} = \frac{1}{Q^\circ b P_s} + \frac{1}{Q^\circ}\ \left(\frac{p}{P_s}\right) \tag{2}$$

and can be fitted to the experimental data using a linear least squares regression. The computer program can solve for the parameters in the model and can also calculate a correlation coefficient, r, which is a measure of the goodness of fit. The computer program generates tables of the raw data, the Langmuir model parameters, and generates plots of both the data and best fit Langmuir isotherms.

Statistical Methods

A linear correlation was assumed between $\ell n\ Q^\circ b$ and $\Delta G^{\text{asssoc}}_{\text{solvent}}$, NET, TSA and MW. The correlation coefficient, r, is a test of the intensity of the linear association between two variables [20]. When r is equal to zero the variables are not linearly correlated. When r approaches plus or minus one the variables are highly linearly correlated. The absolute value of r is used in all of the following discussions. If our variables are x and y we calculate r as

$$r = \Sigma(x_i - \bar{x})(y_i - \bar{y})/[\Sigma(x_i - \bar{x})^2\ \Sigma(y_i - \bar{y})^2]^{1/2} \tag{3}$$

where $\bar{x}$ and $\bar{y}$ are the means of x and y and i indicates the i^{th} point in the summation over n points.

If the equality of correlation coefficients are to be tested, then the confidence limits at various confidence values, $1 - 2\alpha$, can be calculated. First the r value is converted to a z value [21]

$$z = \tanh^{-1} r = \frac{1}{2}\ \ell n\ \left[\frac{1+r}{1-r}\right] \tag{4}$$

The confidence limits for the correlation coefficient are [21]

$$\text{Prob}\left[\tanh\left(z - |C_\alpha|\,\sigma_z\right) \leq r \leq \tanh\left(z + |C_\alpha|\,\sigma_z\right)\right] \qquad (5)$$

$$= 1 - 2\alpha$$

where σ_z is related to the number of points

$$\sigma_z = \sqrt{\frac{1}{n-3}} \qquad (6)$$

and C_α can be found in statistical tables as a function of α [21].

SECTION 5

THEORETICAL

General Solvophobic Approach

Conceptually, solute adsorption onto activated carbon may be represented by the following reversible association reaction

$$S_i + C \rightleftharpoons S_iC \qquad (7)$$

where S_i is the adsorbing solute, C is the activated carbon, and S_iC is the adsorbed solute-carbon complex. The equilibrium constant for this reaction, $K_{solvent,i}$, is related to the overall free energy change, $\Delta G^{assoc}_{solvent}$ by

$$\Delta G^{assoc}_{solvent} = -RT \ln K_{solvent,i} \qquad (8)$$

The solvophobic theory (cϕ) takes into account the effect of the solvent on the above association reaction by considering two hypothetical steps. First, a cavity in the solvent must be created to contain the reacting species. Second, after the gas phase reaction, the "molecules" are placed into the cavities, where each species may interact with the surrounding solvent. This process is depicted in Figure 3.

The overall free energy change may then be calculated as the sum of the free energy changes of the gas phase reaction and the effect of the solvent

$$\Delta G^{assoc}_{solvent} = \Delta G^{assoc}_{gas} + \Delta G^{net}_{solvent\ effect} \qquad (9)$$

The solvent effect is due to the interaction of each species with the solvent

$$\Delta G^{net}_{solvent\ effect} = \sum_j \{\Delta G^{net}_{j,S_iC} - \Delta G^{net}_{j,S_i} - \Delta G^{net}_{j,C}\} \qquad (10)$$

where subscript j represents all possible interactions. In previous applications of the solvophobic theory [10-12, 22-28] the interactions considered

ASSOCIATION REACTION

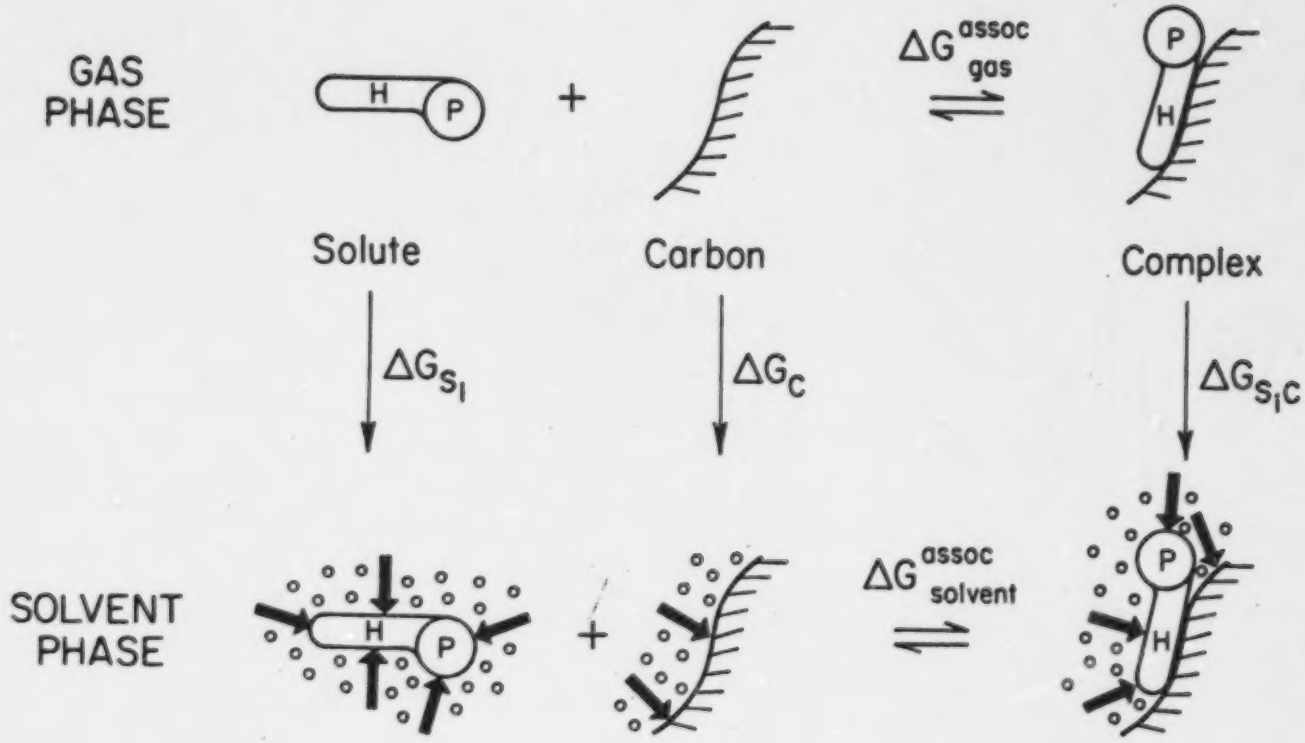

Figure 3. Association adsorption reaction

were cavity formation, van der Waals dispersion (including reduction due to the presence of a solvent), and electrostatic interactions. Combining Eqs. (9) and (10) gives

$$\Delta G^{\text{assoc}}_{\text{solvent}} = \Delta G^{\text{assoc}}_{\text{gas}} + [\Delta G_{\text{cav}} + \Delta G_{\text{vdw}} + \Delta G_{\text{es}}]^{\text{net}}_{S_i C - S_i - C}$$

$$- RT \ln(RT/P_o V) \qquad (11)$$

The free energy change for cavity formation can be calculated for species i as [22]

$$\Delta G_{\text{cav},i} = \gamma_i A_i \kappa_i^e (1 - W) N_a \qquad (12)$$

where W is given by,

$$W = \left(1 - \frac{\kappa_i^e}{\kappa_i^s}\right) \left(\frac{d \ln \gamma}{d \ln T} + \frac{2}{3} \tilde{a}_i T\right). \qquad (13)$$

The van der Waals' interaction is represented by an effective Kihara potential (a modified Lennard-Jones potential). The term "effective" refers to the fact that it is corrected due to presence of surrounding solvent. This potential is integrated over a discrete solvent layer, then an outer solvent continuum. The resulting approximate equation is [23]

$$\Delta G_{\text{vdw},i} \approx \Delta_i D_i D (0.606\ Q) \qquad (14)$$

where

$$\Delta_i = \frac{1.35\ I_i I}{I_i + I}; \qquad D_i = \frac{n_{D,i}^2 - 1}{n_{D,i}^2 + 2} \qquad (15,16)$$

for solute i, nonsubscripted variables refer to the solvent. Also,

$$Q = \nu_i \left[\frac{\overline{\sigma^6}}{(\overline{R} - \overline{T})^9} \left(\frac{t^2}{11} + \frac{t}{5} + \frac{1}{9}\right) - \frac{1}{(\overline{R} - \overline{T})^3} \left(\frac{t^2}{5} + \frac{t}{2} + \frac{1}{3}\right) \right] \qquad (17)$$

where

$$t = \frac{\overline{T}}{(\overline{R} - \overline{T})} \; ; \quad R_i = 1.74 \left(\frac{3\nu_i}{4\pi}\right)^{1/3} ; \quad l_i = R_i \left(\frac{0.24 + 7\omega_i}{3.24 + 7\omega_i}\right) \qquad (18\text{-}20)$$

$$\sigma_i = \left(\frac{3\nu_i}{4\pi}\right)^{1/3} \frac{4.64}{3.24 + 7\omega_i} \qquad (21)$$

and where the bars denote averages.

The electrostatic interactions may be estimated by [25]

$$\Delta G_{es,i} = -\frac{Na}{2} \frac{\mu_i^2}{\nu_i} DP \qquad (22)$$

where

$$D = \frac{2(\varepsilon - 1)}{2\varepsilon + 1} \qquad (23)$$

and

$$P = \left[4\pi\varepsilon_o \left(1 - \frac{D\alpha_i}{\nu_i}\right)\right]^{-1} \qquad (24)$$

Substituting Eqs. (12) -(24) into (11) gives

$$\Delta G^{\text{assoc}}_{\text{solvent}} = \Delta G^{\text{assoc}}_{\text{gas}} + [\Delta G_{\text{vdw},S_i,C} - \frac{N_a}{2} \frac{\mu^2_{S_iC}}{\nu_{S_iC}} DP$$

$$+ N_a \kappa^e_{S_iC} A_{S_iC} \gamma_{w,S_iC}(1 - W_{S_iC})]$$

$$- [\Delta G_{\text{vdw},S_i} - \frac{N_a}{2} \frac{\mu^2_{S_i}}{\nu_{S_i}} DP + N_a \kappa^e_{S_i} A_{S_i} \gamma_{w,S_i}(1 - W_{S_i})]$$

$$- [\Delta G_{\text{vdw},C} - \frac{N_a}{2} \frac{\mu^2_C}{\nu_{S_i}} DP + N_a \kappa^e_C A_C \gamma_{w,C}(1 - W_C)]$$

$$- RT \ln(RT/P_o V) \qquad (25)$$

At this point, all of the considered solvent-solute interactions are included in the general Eq. (25). However, further simplification is needed to make the problem tractable.

With respect to the activated carbon surface, essentially two types of interactions are thought to predominate. The first type of surface interaction, which occurs on most of the available surface area (on basal planes) can be characterized by van der Waals' physical interactions, and is apolar in nature. The second type of surface interaction which occurs at the more reactive edges of the microcrystallites, and at surface functional groups, can be characterized by physical (and maybe even chemical) attractive interactions due to electrostatic effects. Although the second type of surface interaction occurs at a small fraction of the total surface area, adsorption differences between different activated carbons is probably the result of their energy potential distributions, and extent of surface functional groups. However, since hydrophobic or apolar interactions play a dominant role in activated carbon adsorption of nonpolar (or nonpolar moieties of) solutes, only the first type of surface interaction discussed above will be considered here.

Considering the carbon surface to be nonpolar, the following assumptions can be made, $\mu_C = 0$ (nonpolar carbon); $\mu_{S_iC} = \mu_{S_i}$ (solute could be polar); $\Delta G_{\text{vdw},S_iC} = \Delta G_{\text{vdw},C}$ (dilute range).

In addition, since the carbon surface is much larger than the solute, then [25]

$$W_{S_iC} = W_{S_i} = W_C \text{ and } \kappa^e_{S_iC} = \kappa^e_C = 1$$

Also per Horvath

$$\kappa^e_{S_i} \approx 1 + (\kappa^e - 1)(V/V_{S_i}) \tag{26}$$

where κ^e is the microscopic cavity factor for pure water, and has a value of 1.277 [23].

To simplify the algebra, the molecular volume of the carbon-solute complex S_iC may be expressed as a multiple of the solute molecular volume,

$$\nu_{S_iC} = \lambda \nu_{S_i} \tag{27}$$

where λ is the proportionality constant. For high pressure liquid chromatography, λ was estimated to be approximately 3.7. Since the carbon-solute complex S_iC is much larger than the solute S_i, λ is arbitrarily chosen as $\lambda = 100$ for this work. Previously, it was shown that the actual value of λ has only a very weak effect on $\Delta G^{assoc}_{solvent}$.

Finally, because of the association adsorption reaction of solute S_i onto adsorbent C, the total surface area in contact with the free solvent is reduced by,

$$\Delta A = A_{S_i} + A_C - A_{S_iC} \tag{28}$$

ΔA has been termed "the thermodynamic microsurface area change of reaction" [24].

Substituting the above assumptions into Eq. (25) gives

$$\Delta G^{\text{assoc}}_{\text{solvent}} = \Delta G^{\text{assoc}}_{\text{gas}} - \Delta G_{\text{vdw},S_i} + \frac{N_a\,(\lambda - 1)}{2\lambda}\,\frac{\mu^2_{S_i}}{\nu_{S_i}}\,DP$$

$$- N_a\gamma\Delta A - N_a\gamma V^{2/3}(\kappa^e - 1)\,\frac{A_{S_i}}{V^{2/3}_{S_i}} - RT\,\ln\frac{RT}{P_o V} \qquad (29)$$

Eq. (29) may be further simplified by noting that in the fifth term on the right hand side, $A_{S_i}/V^{2/3}_{S_i}$ is a constant for a given molecular shape. Therefore, for spherical molecules,

$$A_{S_i} = 4.836\,\nu^{2/3}_{S_i} = 4.836\,(V_{S_i}/N_a)^{2/3} \qquad (30)$$

and Eq. (29) becomes,

$$\Delta G^{\text{assoc}}_{\text{solvent}} = \Delta G^{\text{assoc}}_{\text{gas}} - \Delta G_{\text{vdw},S_i} + \frac{N_a(\lambda - 1)}{2\lambda}\,\frac{\mu^2_{S_i}}{\nu_{S_i}}\,DP$$

$$- N_a\gamma\Delta A - 4.836\,N_a^{1/3}\,\gamma(\kappa^e - 1)V^{2/3} - RT\,\ell n\frac{RT}{P_o V} \qquad (31)$$

The free energy change of the association reaction is related to its equilibrium constant by Eq. (8). At low concentrations $K_{\text{solvent, i}}$ is proportional to the initial slope of the aqueous phase adsorption isotherm. If we use a Langmuir isotherm model the initial slope is Q°b. Until now the gas phase term in Eq. (31) has been assumed constant for a homologous series of organics. If this assumption is made and Eqs. (8) and (31) are combined, then

$$\ln Q°b \propto \frac{\Delta G_{\text{vdw},S_i}}{RT} - \frac{N_a(\lambda - 1)}{2\lambda RT}\,\frac{\mu^2_{S_i}}{\nu_{S_i}}\,DP$$

$$+ \frac{\gamma}{RT}\left(N_a \Delta A + 4.836\, N_a^{1/3}(\kappa^e - 1)V^{2/3}\right) + \ln \frac{RT}{P_o V} \qquad (32)$$

This can be written more simply as

$$\ln Q°b \propto - \Delta G^{\text{net}}_{\text{solvent effect}}/RT \qquad (33)$$

The solvophobic theory may be simplified further [10-12] to obtain the result that ln Q°b should be proportional to the total surface area of the solute molecule (abbreviated TSA).

Thermodynamic of Gas Phase Adsorption

The objective here is to obtain an expression for estimating $\Delta G^{\text{assoc}}_{\text{gas}}$ for adsorption of solutes from the vapor phase. The values of $\Delta G^{\text{assoc}}_{\text{gas}}$ calculated for each solute can then be correlated *ipso facto* for gas-phase adsorption and also be used in Eqs. (9) or (31) to obtain a complete expression for $\Delta G^{\text{assoc}}_{\text{solvent}}$ for liquid-phase adsorption. $\Delta G^{\text{assoc}}_{\text{gas}}$ can be calculated by first finding the change in surface free energy of adsorption of a gas onto the activated carbon surface. The spreading pressure, π is the reduction in the surface free energy of a solid surface due to vapor adsorption. The free energy change of adsorption can be calculated by multiplying the spreading pressure by the molar area occupied by the adsorbate in a surface layer, a_i

$$-\Delta G^{\text{assoc}}_{\text{gas}} = a_i \pi \qquad (34)$$

The spreading pressure can be expressed as [15]

$$\pi = \gamma_s - \gamma_{sg} \qquad (35)$$

or by using Young's equation as

$$\pi = \gamma_s - \gamma_{s\ell} - \gamma_\ell \cos\theta \qquad (36)$$

If $\theta \approx 0$ a spreading system is obtained and:

$$\pi = \gamma_s - (\gamma_\ell + \gamma_{s\ell}) \tag{37}$$

Fowkes [15] gives an expression for the interfacial tension between solid and liquid as

$$\gamma_{s\ell} = \gamma_s + \gamma_\ell - 2\sqrt{\gamma_s^d \gamma_\ell^d} \tag{38}$$

where d indicates the London dispersion contribution to the overall surface free energy. For adsorbate species i

$$\gamma_i^d = \frac{-\pi N_i^2 \alpha_i^2 I_i}{8\, r_{ii}^2} \tag{39}$$

where

$$N_i = \nu_i^{-1} = \left(\frac{MW}{N_a \rho_i}\, 10^{24}\right)^{-1} \tag{40}$$

$$\alpha_i = \frac{3}{4}\frac{\nu_i}{\pi}\left[\frac{n_D^2 - 1}{n_D^2 + 2}\right] \tag{41}$$

$$r_{ii} \approx \left(\frac{6\nu_i}{\pi}\right)^{1/3} \tag{42}$$

r_{ii} is estimated assuming spherical molecules. It should be noted that Eq. (42) overestimates the interatomic distance, thus underestimating the dispersion force in Eq. (39). The general trend in the values is still maintained however providing consistent relative results.

Combining Eqs. (34), (37), and (38) the free energy for adsorption from the vapor phase is obtained

$$\Delta G^{\text{assoc}}_{\text{gas}} = 2a_i(\gamma_\ell - \sqrt{\gamma_s^d \gamma_\ell^d}) \qquad (43)$$

where the molar area for closest hexagonal packing of spherical molecules on the surface is,

$$a_i = \frac{\sqrt{3}}{2} r_{ii}^2 N_a \qquad (44)$$

and the Parachor, [P], is used to estimate γ_ℓ [29,30]

$$\gamma_\ell = \{[P] \frac{\rho_i}{MW}\}^4 \qquad (45)$$

Converting Eqn. (43) into dimensionless form at 293°K and evaluating the known constants, obtains

$$\Delta G^{\text{assoc}}_{\text{gas}}/RT = (4.2804 \times 10^{-3}) r_{ii}^2 [\gamma_\ell - \sqrt{\gamma_s^d \gamma_\ell^d}] \qquad (46)$$

where all that remains is to obtain an estimate of γ_s^d for the specific activated carbon sorbent used in the study. Two methods using vaporphase isotherms to obtain a value for γ_s^d are presented below.

The first method to estimate the value of γ_s^d uses the low pressure data of the adsorption isotherm. Since the data available in this study fit the Langmuir model fairly well, a dimensionless form of the Langmuir equation can be used

$$q/Q^\circ = \frac{b(p/p_s)}{1/p_s + b(p/p_s)} \qquad (47)$$

Taking the initial slope of this isotherm

$$\left.\frac{d(q/Q^\circ)}{d(p/p_s)}\right|_{p/p_s \to o} = bp_s \qquad (48)$$

to obtain an estimate of the equilibrium constant $K_{gas,i} = bp_s$. We can now write an equation analogous to Eqs. (8) and (33) but for gas phase adsorption.

$$\Delta G^{assoc}_{gas}/RT = - \ell n\, K_{gas,i} \approx - \ell n\, bp_s \qquad (49)$$

Equating Eqs. (46) and (49), and using Eqs. (39) - (45), a mean value for γ_s^d can be obtained from the gas phase isotherms of several solutes.

The second method to estimate the value of γ_s^d uses the entire gas phase isotherm. The Gibbs adsorption isotherm is given by [15]

$$d\gamma = -\Gamma RT\, d\, \ell n\, p \qquad (50)$$

Γ is the areal surface excess given by

$$\Gamma = q/A \qquad (51)$$

where A is the specific surface area of the adsorbent (m^2/g).
Integrating Eq. (50) from zero pressure to saturation pressure gives

$$\int_{\gamma_s}^{\gamma_{sg}} d\gamma = - \frac{RT}{A} \int_o^{p_s} q\, d\, \ell n\, p \qquad (52)$$

Substituting for q from Eqn. (47) obtains

$$\gamma_{sg} - \gamma_s = - \frac{RTQ^\circ b}{A} \int_o^{p_s} \frac{dp}{(1+bp)} \qquad (53)$$

or with Eqn. (35) and integration, obtains

$$\pi_e = \frac{RTQ^\circ}{A} \ln (1 + bp_s) \tag{54}$$

Finally, combining Eqs. (37) and (38) obtains

$$\gamma_s^d = (\pi_e + 2\gamma_\ell)^2/4\gamma_\ell^d \tag{55}$$

which, when used with Eq. (54) gives an estimate of γ_s^d.

Surface Tensions and Aqueous Adsorption

For a given solute, when the solvent composition is changed at a constant temperature, we can assume that the solute and carbon properties as well as ΔG_{gas}^{assoc} are constant. Hence Eq. (32) can be written as [25]:

$$\ln Q^\circ b \propto C_1 D + C_2 \gamma + C_3(\kappa^e - 1) V^{2/3}\gamma + \ln\left(\frac{RT}{P_o V}\right) \tag{56}$$

where the constants are given by

$$C_1 = \frac{1}{RT} \frac{1-\lambda}{2\lambda} \frac{\mu_{S_i}^2}{\nu_{S_i}} N_a P \tag{57}$$

$$C_2 = \frac{N_a \Delta A}{RT} \tag{58}$$

$$C_3 = 4.836\ N_a^{1/3}/RT \tag{59}$$

If it is assumed that D≈1 and the solvent molar volume changes slightly when compared with the surface tension then Eq. (56) simplifies to:

$$\ell n\ Q^{\circ}b \propto C_2\gamma + C_4(\kappa^e - 1)\gamma \tag{60}$$

where

$$C_4 = 4.836\ N_a^{1/3}\ V^{2/3}/RT \tag{61}$$

If the parameter κ^e remains constant a final simplification can be made:

$$\ell n\ Q^{\circ}b \propto C_5\gamma \tag{62}$$

where

$$C_5 = \frac{N_a\Delta A + 4.836\ N_a^{1/3}\ V^{2/3}(\kappa^e - 1)}{RT} \tag{63}$$

If the adsorption parameters for the solute in pure water are known, then

$$\ell n\ Q^{\circ}b = \ell n(Q^{\circ}b)_o + C_5(\gamma-\gamma_o) \tag{64}$$

where $(Q^{\circ}b)_o$ is the initial slope of the isotherm for adsorption from pure water, and γ_o is the surface tension of pure water (=72 ergs/cm^2). The surface tension of inorganic salt solutions in water can usually be expressed as a linear function of salt concentration [25]

$$\gamma = \gamma_o + \tau m \tag{65}$$

where m is the molal salt concentration and τ is a coefficient which depends on the salt (=2.17 for $(NH_4)_2SO_4$). Combining Eqs. (64)nd (65) obtains

$$\ell n\ Q^{\circ}b = \ell n(Q^{\circ}b)_o + C_5\tau m \tag{66}$$

A plot of $\ell n\ Q^{\circ}b$ vs. salt concentration should therefore yield a straight line with a slope equal to $C_5\tau$.

For the case of mixed organic solvents the surface tension is probably not a linear function of concentration so an expression such as Eq. (60) or (62) must be used.

Multicomponent Adsorption

The Ideal Adsorbed Solution (IAS) theory approaches multicomponent adsorption as a classical thermodynamic phase equilibrium problem, equating the chemical potential of the ith species in the bulk solution to its chemical potential in the adsorbed phase. By assuming that the adsorbed phase forms an ideal solution (6), the following system of equations are obtained:

$$C_i(\pi,T,Z_i) = Z_i C_i^\circ(\pi,T) \tag{67}$$

$$\pi_i = \frac{RT}{A}\int_0^{C_i^\circ} \frac{Q_i}{C_i}\, dC_i^\circ \tag{68}$$

$$Q_i^\circ = g_i(C_i^\circ) \tag{69}$$

$$\frac{1}{Q_T(\pi,T)} = \sum_{i=1}^{n} \frac{Z_i}{Q_i^\circ(\pi,T)} \tag{70}$$

$$Z_i Q_T = Q_i \tag{71}$$

$$\sum_{i=1}^{n} Z_i = 1 \tag{72}$$

$$\pi_i = \pi_j = \pi \tag{73}$$

Note that the summation in Eqs. (70) and (72) are over solute species only. Once the dependence of Q_i° on C_i° is known, whether by an isotherm equation or from experimental data, the remaining equations may be solved.

However, predicted adsorption equilibria are not always found to be in good agreement with experimental data. Both competition for the active centers of the solid surface and interaction between adsorbed molecules occurs. Therefore the ideal adsorbed solution theory can be refined by modifying Raoult's law with a two-dimensional equation of state to specify the actual state in the adsorbed phase.

It is useful to define an adsorbed-phase fugacity $\hat{f}_i^a$ according to (31)

$$d\mu_i^a = RT\, d\ln \hat{f}_i^a \quad \text{(constant T)} \tag{74}$$

and

$$\lim_{\pi \to 0} \frac{\hat{f}_i^a}{Z_i \pi} = 1 \quad \text{(constant T)} \tag{75}$$

where the adsorbed-phase mole fraction is defined by

$$Z_i = \frac{Q_i}{\sum_{i=1}^{n} Q_i} = \frac{Q_i}{Q_T} \tag{71}$$

The adsorbed-phase fugacity is two-dimensional and has the same units as the spreading pressure π.

Equilibrium between an adsorbate and a liquid phase requires:

$$\mu_i = \mu_i^a \quad \text{and} \quad d\mu_i = d\mu_i^a \tag{76}$$

For each phase we have the expressions:

$$d\mu_i = RT\, d\ln \hat{f}_i \quad \text{(constant T)}$$

$$d\mu_i^a = RT\, d\ln \hat{f}_i^a \quad \text{(constant T)}$$

Thus we may write:

$$d\ln \hat{f}_i = d\ln \hat{f}_i^a \quad \text{(constant T)}$$

Integration at constant temperature from an equilibrium state of single solute i at very low spreading pressure π_i^* in the adsorbate and very low con-

centration C_i^* in the bulk solution to the equilibrium state of interest where i has mole fraction Z_i at spreading pressure π in the adsorbate and concentration C_i in the bulk solution gives:

$$\ln \frac{\hat{f}_i(C_i)}{f_i(C_i^*)} = \ln \frac{\hat{f}_i^a(\pi)}{f_i^a(\pi^*)}$$

or

$$\hat{f}_i^a(\pi) = \frac{\hat{f}_i(C_i)}{f_i(C_i^*)} \cdot f_i^a(\pi_i^*) \tag{77}$$

Assuming the bulk solution is ideal, then

$$\frac{\hat{f}_i(C_i)}{f_i(C_i^*)} = \frac{C_i}{C_i^*}$$

and

$$\hat{f}_i^a(\pi) = \frac{C_i}{C_i^*} \cdot f_i^a(\pi^*_i) \tag{78}$$

If we let π_i^* and C_i^* approach zero, then $f_i^a(\pi_i^*) \to \pi_i^*$ and the relation between fugacities at equilibrium becomes:

$$\hat{f}_i^a(\pi) = \left(\frac{\pi_i^*}{C_i^*}\right) \cdot C_i \tag{79}$$

At very low spreading pressures the ideal-gas analog equation becomes valid. Thus, $\pi_i^* a_i^* = RT$, or alternatively:

$$\pi_i^* A = O_i^* RT$$

or

$$\frac{O_i^*}{A} = \frac{\pi_i^*}{RT}$$

where a and A are molar surface area and surface area per gram of adsorbent, respectively.

The analogue Henry's constant, K_i, is given by:

$$K_i = \frac{1}{A}\left(\frac{dQ_i}{dC_i}\right)^* = \frac{1}{A}\lim_{C_i \to 0}\left(\frac{Q_i}{C_i}\right) = \frac{1}{A}\frac{Q_i^*}{C_i^*}$$

Thus, $\frac{\pi_i^*}{RT} = K_i C_i^*$ and Equation (79) now becomes:

$$\hat{f}_i^a(\pi) = K_i RTC_i \qquad (80)$$

K_i is a function of temperature only for a given adsorbent and substrate. It is a quantity which characterizes the specific interaction between a particular adsorbed species and a particular substrate.

Several two-dimensional equations have been proposed for pure components in gas phase adsorption; one that has received particular attention is the two-dimensional analogue of van der Waals' equation (32):

$$\pi = \frac{RT}{a-\beta} - \frac{\alpha}{a^2} \qquad (81)$$

where α and β represent the interaction between adsorbed species and the surface area occupied by adsorbate, respectively.

For a binary-solute mixture, we assume that the constants α and β are related to those of the pure components by a pair of the "mixing rules" - i.e., equations expressing α and β as functions of composition. One pair of rules which has proved useful for a binary system is (33):

$$\beta = Z_1\beta_1 + Z_2\beta_2 \qquad (82)$$

and

$$\alpha = Z_1^2\alpha_1 + 2Z_1Z_2\alpha_{12} + Z_2^2\alpha_2 \qquad (83)$$

where α_{12} is a constant characteristic of the 1-2 interaction. Following Hoory and Prausnitz (34), we assume that $\alpha_{12} = \sqrt{\alpha_1\alpha_2}$.

The calculation of the fugacity of a mixed adsorbate at fixed temperature and composition using the two-dimensional analogue of van der Waals' equation was derived by Van Ness (33):

$$\ln \hat{f}_1^a = \ln \frac{Z_1 RT}{a-\beta} + \frac{\beta_1}{a-\beta} - \frac{2}{aRT}(\alpha_1 Z_1 + \alpha_{12} Z_2) \tag{84a}$$

$$\ln \hat{f}_2^a = \ln \frac{Z_2 RT}{a-\beta} + \frac{\beta_2}{a-\beta} - \frac{2}{aRT}(\alpha_2 Z_2 + \alpha_{12} Z_1) \tag{84b}$$

Eliminating $\hat{f}_1^a$ and $\hat{f}_2^a$ with Equation (80):

$$\ln C_1 = \ln \frac{Z_1}{K_1(a-\beta)} + \frac{\beta_1}{a-\beta} - \frac{2}{aRT}(\alpha_1 Z_1 + \alpha_{12} Z_2) \tag{85a}$$

$$\ln C_2 = \ln \frac{Z_2}{K_2(a-\beta)} + \frac{\beta_2}{a-\beta} - \frac{2}{aRT}(\alpha_2 Z_2 + \alpha_{12} Z_1) \tag{85b}$$

By assigning values to the constants α_1, α_2, α_{12}, β_1, β_2, K_1, and K_2 from single solute isotherms, these equations can be solved for Z_1, Z_2, and a for any values of C_1 and C_2 in a binary mixture.

SECTION 6

RESULTS AND DISCUSSION

Comparison Between Different Carbons

In Figs. 4 and 5, the adsorption capacity ($\ln Q°b$) versus molecular weight (MW) or cavity surface area (TSA) for linear alcohols on different carbons are plotted, respectively. $Q°b$ is Henry's constant, i.e., the slope of Q versus C at infinite dilution. As the concentration, C, of the solute approaches zero, so Q, the amount adsorbed per mass of carbon, divided by C approaches $Q°b$.

In Table 2, the Langmuir adsorption parameters $Q°$ and $\ln Q°b$ are correlated for the linear alcohols with molecular weight. Very good correlations are obtained. In order to test the simplified version of the solvophobic theory for different carbons, the molecular cavity surface area of each solute (i.e., the total surface area, TSA) was calculated using the MDS program (35). The TSA for each alkyl alcohols is then correlated with the Langmuir adsorption parameters in an attempt to verify the theory as a predictive measure of solute adsorption. In Table 2, we observe the adsorptivities for the linear alcohols also correlate well with TSA. However, TSA, does not significantly correlate with adsorption parameters any better than molecular weight for linear alcohols, as expected.

In Table 3, the Langmuir adsorption parameters $Q°$ and $\ln Q°b$ are listed with characteristics of adsorbents for five different carbons. Both the saturation adsorption and adsorption capacity have no apparent correlation with surface area of adsorbents. The surface energy of adsorbent should have an important effect on the adsorption process.

The Differences Between Gas and Liquid Phase Adsorption

Adsorption isotherms were measured in the gas phase and in the liquid phase for four linear alcohols (butanal-heptanol) and three branched alcohols (2-methyl 1-butanol, 2-methyl 3-pentanol, 3-3-dimethyl 1-butanol) on the same activated carbon. All of these isotherms fit the Langmuir form very well and the parameters of this model versus molecular weight of the linear alcohol are shown in Figure 6. The saturated adsorption capacity, $Q°$, increases linearly with molecular weight for adsorption from solution while the opposite is seen for gas adsorption. The amount of water adsorbed from the aqueous phase can also be estimated by assuming complete wetting of the entire carbon surface ($1014\ m^2/g$). Assuming spherical molecules in hexagonal packing on the surface, the amount of water necessary to cover the remaining surface, not covered by the alcohol, can be calculated. The adsorption capacity for water is also shown on Figure 6 and is seen to decrease linearly as the alcohol adsorption increases. Since the water curve is much higher than the solute curve we know that the solute never forms a complete monolayer on the surface in liquid phase adsorption. The energy term, b, increases with molecular weight in all cases except one. The anomalous result for the adsorption of heptanol from the gas phase is probably caused by steric exclusion effects or

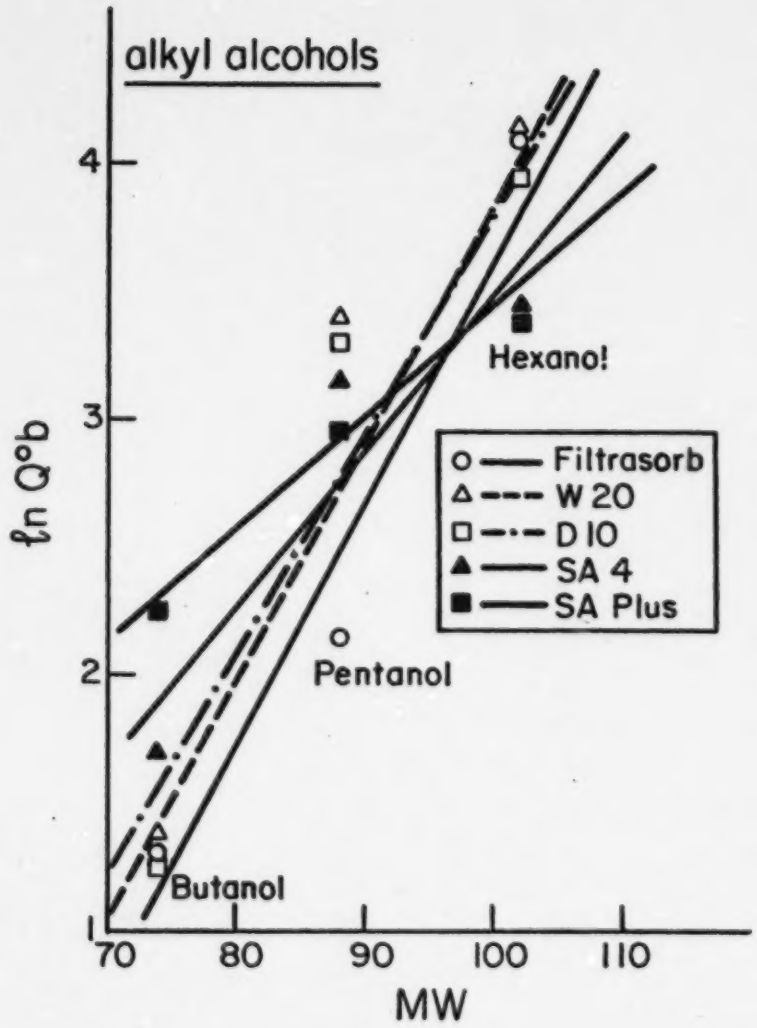

Figure 4. Adsorbability (lnQ°b) versus MW for linear alcohols

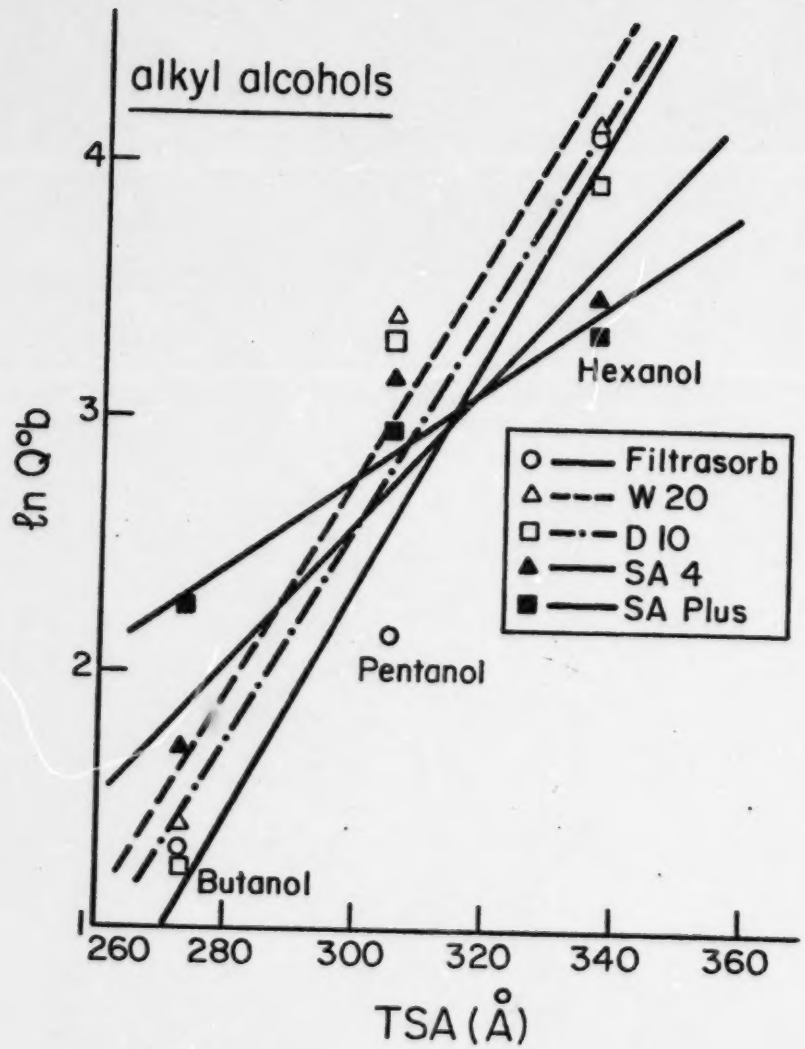

Figure 5. Adsorbability (lnQ°b) versus cavity surface area for linear alcohols

TABLE 2

Correlation Coefficient r for Langmuir Adsorption Parameters vs. Molecular Weight and Total Surface Area for the Alkyl Alcohols on Five Different Carbons[a]

Adsorption	Filtrasorb 400		W20		D10		SA4		SA Plus	
Parameter	Molecular Weight	TSA A^2	Molecular Weight	TSA A^2	Molecular Weight	TSA A^2	Molecular Weight	TSA A^2	Molecular Weight	TSA A^2
Q°	0.99	0.99	0.85	0.85	0.87	0.87	0.79	0.79	0.99	0.99
lnQ°b	0.97	0.97	0.96	0.94	0.97	0.97	0.93	0.93	0.98	0.98

[a] The alcohols studied were butanol, pentanol and hexanol.

TABLE 3

Langmuir Adsorption Parameters for the Alkyl Alcohols on Five Different Carbons

Adsorbents	Surface Area (m^2/g)	Iodine Adsorption (mg/g)	Butanol		Pentanol		Hexanol	
			$\ln Q°b$	$Q°$ (mmoles/g)	$\ln Q°b$	$Q°$ (mmoles/g)	$\ln Q°b$	$Q°$ (mmoles/g)
Filtrasorb	1031	1200	1.29	0.18	2.14	0.44	4.12	0.78
W20	540	590	1.36	0.50	3.41	0.49	4.16	0.73
D10	530	580	1.25	0.55	3.31	0.62	3.93	0.62
SA4	690	715	1.68	0.61	3.16	0.56	3.42	0.91
SA Plus	930	1040	2.23	0.35	2.96	0.60	3.30	0.86

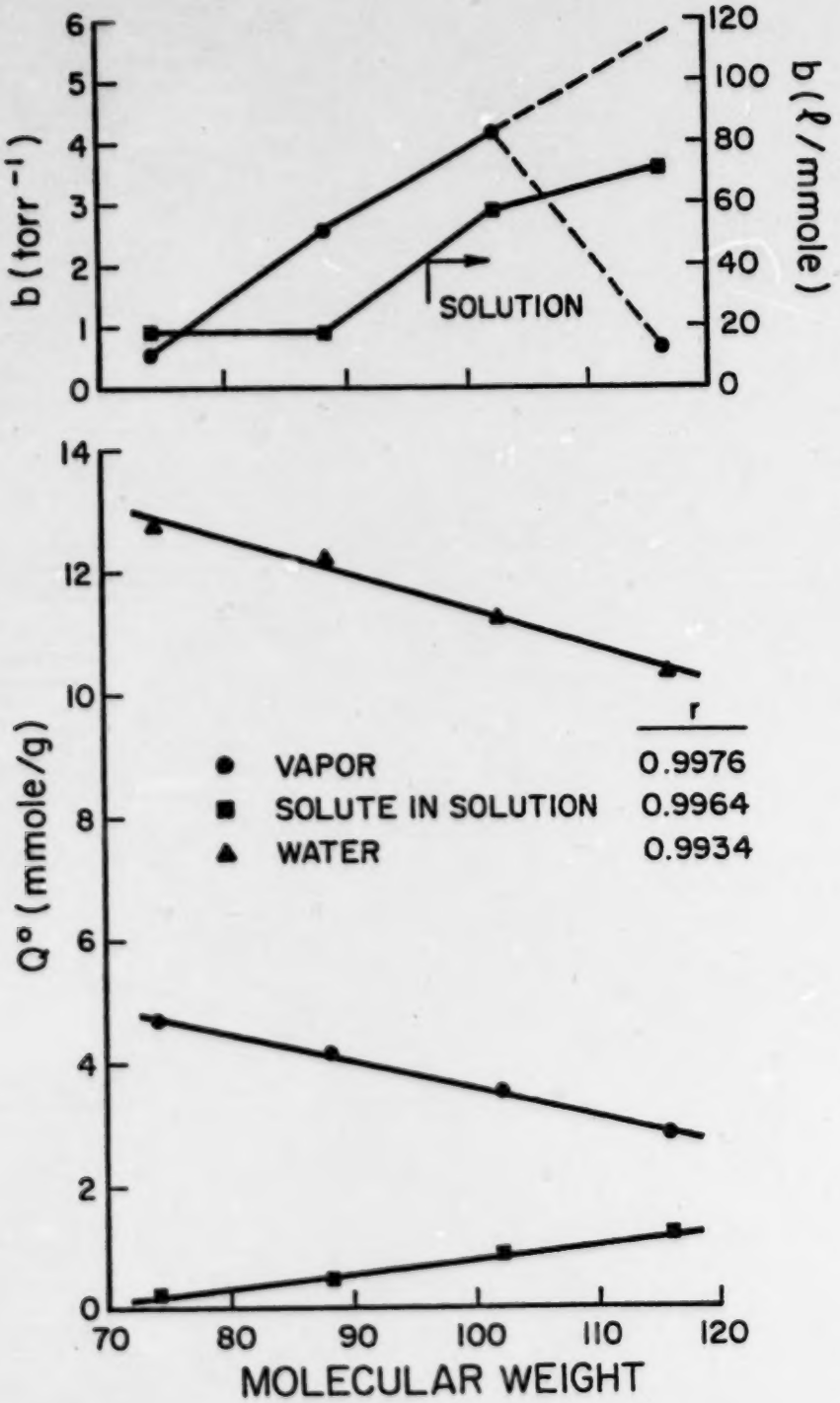

Figure 6. Langmuir model parameters versus molecular weight for the adsorption of linear alcohols from gas and liquid phases.

incomplete adsorption since extreme hysteresis was observed for its isotherm during desorption. Estimating a value of b = 18.3 for the water from Figure 6 we can calculate the Henry's Law constant, Q°b, (the slope of the adsorption isotherm at infinite dilution) for water adsorption. The plots of ℓn Q°b for both the water and solute in solution are shown in Figure 1 as a function of the solute molecular weight. Thus, both for the dilute concentration region (ℓn Q°b plot in Figure 7) and the saturation concentration region (Q° plot in Figure 6), increasing solute size displaces an increasing amount of water from the surface.

The gas phase data presented above may be used to calculate the dispersion contribution to the total surface free energy of the activated carbon, γ_s^d, as shown by the two methods prsented in the theoretical section. The results using Eqs. (39) - (49) and Eqs. (54) - (55) are given in Table 4. The results from the two methods are remarkably close to one another (< 3% difference) considering the first method uses only the low pressure data and the second uses the entire adsorption isotherm. It should be noted that the calculated values of γ_s^d are probably too large since, as stated previously, the values for γ_ℓ^d are underestimated. The values of γ_s^d based on the entire isotherm (319.1 ergs/cm^2) is preferable for use in the following free energy calculations.

Next, the overall solvophobic theory developed in the theoretical section may be tested against the experimental data for both liquid and gas phase adsorption.

General Solvophobic Approach

The solvent effect free energies, $\Delta G^{net}_{solvent\ effect}$, for twelve linear and branched alcohols have been calculated previously [11]. The gas phase free energies are calculated using Eqs. (39) - (46) and added to the solvent effect free energies to yield the free energy change in solution (see Eq. (9)). The physical properties needed to calculate ΔG^{assoc}_{gas} can be found in standard references (30,36) and are summarized in Table 5 for the alcohols. The calculated free energies $\Delta G^{net}_{solvent\ effect}/RT$, $\Delta G^{assoc}_{gas}/RT$ and $\Delta G^{assoc}_{solvent}/RT$ are given in Table 6 along with ℓnQ°b measured by Ferrick [37]. These free energies can be abbreviated NET, GAS, and SOLVENT, respectively. Also given in Table 6 are the total surface areas for the alcohol molecules.

Figure 8 shows NET and GAS versus the number of carbon atoms in the alcohol. The lines are drawn through the four linear alcohols and diverge as the

Figure 7. lnQ°b versus solute molecular weight for linear alcohols and water in solution

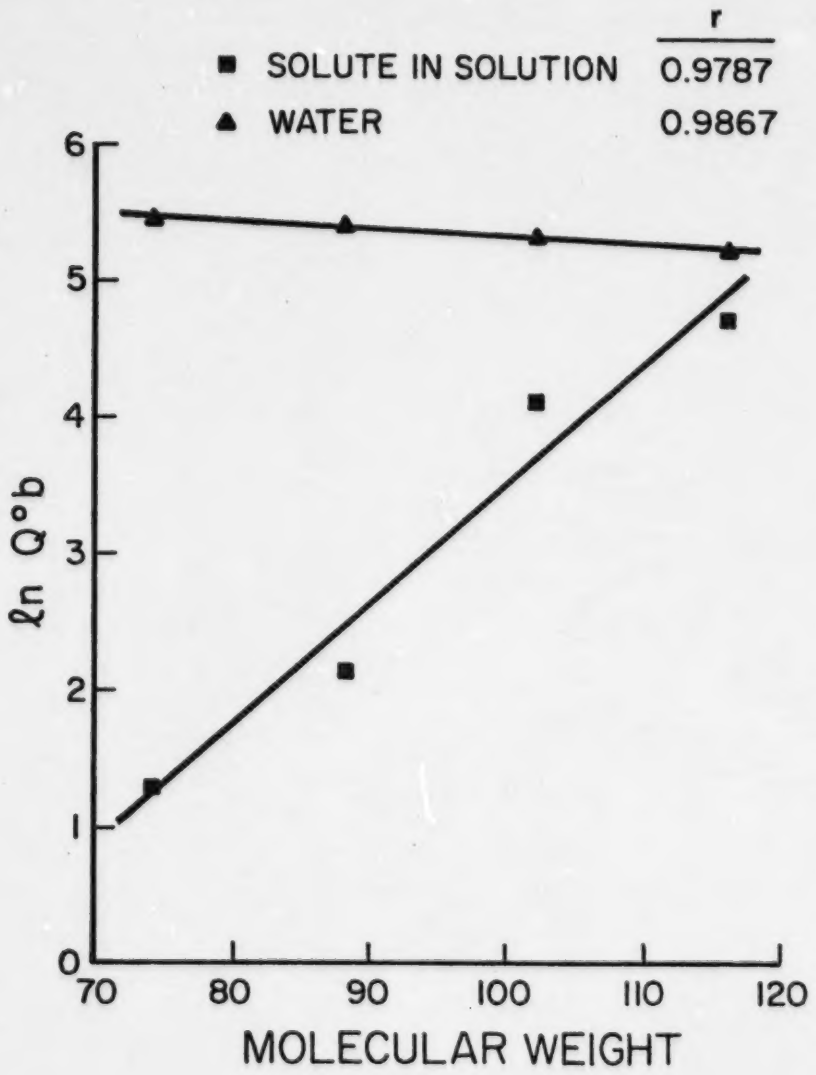

TABLE 4

Calculated Values for γ_s^d for Adsorption of Linear Alcohols Onto Porous Activated Carbon

Compound	γ_s^d (ergs/cm^2) Equations (39)-(49)	γ_s^d (ergs/cm^2) Equations (54)-(55)
1-butanol	291.3	309.7
1-pentanol	318.2	333.7
1-hexanol	334.8	337.6
1-heptanol	302.9	295.4
Average	311.8 ± 18.9	319.1 ± 20.0

TABLE 5

Physical Properties of the Aliphatic Alcohols

compound	MW	ρ (g/cm^3)	ν ($\AA^3$)	r_{ii} ($\AA$)	n_D	α ($\AA^3$)	[P]	γ_ℓ ($\frac{ergs}{cm^2}$)	γ_ℓ^d ($\frac{ergs}{cm^2}$)
1. 1-butanol	74.12	0.8097	152.06	6.622	1.3993	8.787	205.3	24.60	4.796
2. 2-methyl 1-butanol	88.15	0.8191	178.77	6.989	1.4107	10.590	241.6	25.40	4.513
3. 1-pentanol	88.15	0.8148	179.71	7.002	1.4100	10.630	245.3	26.43	4.482
4. 2,3-dimethyl 2-butanol	102.18	0.8226	206.34	7.332	1.4173	12.396	274.2	23.74	4.230
5. 3,3-dimethyl 1-butanol	102.18	0.8147	208.34	7.355	1.4138	12.423	277.9	24.10	4.135
6. 2-ethyl 1-butanol	102.18	0.8281	204.97	7.315	1.4224	12.445	281.6	27.13	4.336
7. 2-methyl 3-pentanol	102.18	0.8239	206.01	7.328	1.4168	12.363	277.9	25.21	4.212
8. 2-methyl 1-pentanol	102.18	0.8130	208.78	7.360	1.4154	12.492	281.6	25.20	4.158
9. 1-hexanol	102.18	0.8198	207.04	7.340	1.4181	12.459	285.3	27.45	4.229
10. 2,4-dimethyl 3-pentanol	116.20	0.8290	232.84	7.633	1.4250	14.213	314.2	25.25	4.014
11. 3-ethyl 3-pentanol	116.20	0.8445	228.57	7.586	1.4301	14.099	317.9	28.49	4.169
12. 1-heptanol	116.20	0.8225	234.68	7.653	1.4241	14.299	325.3	28.11	3.986

TABLE 6

Physical Properties and Solvophobic Contributions for the Alcohols

Adsorbate	MW	TSA ($Å^2$)	ℓn Q°b	$\Delta G^{net\ solvent}/RT$ effect	$\Delta G^{assoc}_{gas}/RT$	$\Delta G^{assoc}_{solvent}/RT$
1. 1-butanol	74.12	251.5	1.29	-2.94	-2.725	-5.67
2. 2-methyl 1-butanol	88.15	267.2	2.54	-6.44	-2.624	-9.06
3. 1-pentanol	88.15	282.2	2.14	-7.69	-2.390	-10.08
4. 2,3-dimethyl 2-butanol	102.18	274.1	1.78	-6.22	-2.991	-9.21
5. 3,3-dimethyl 1-butanol	102.18	284.0	2.07	-9.16	-2.831	-11.99
6. 2-ethyl 1-butanol	102.18	290.0	3.33	-11.17	-2.306	-13.48
7. 2-methyl 3-pentanol	102.18	290.7	3.16	-9.88	-2.632	-12.51
8. 4-methyl 1-pentanol	102.18	300.4	3.52	-12.59	-2.603	-15.19
9. 1-hexanol	102.18	312.9	4.12	-14.28	-2.141	-16.42
10. 2,4-dimethyl 3-pentanol	116.20	301.2	3.45	-13.62	-2.628	-16.25
11. 3-ethyl 3-pentanol	116.20	302.0	3.30	-12.30	-1.967	-14.27
12. 1-heptanol	116.20	343.6	4.72	-20.78	-1.894	-22.67

Figure 8. $\Delta G^{net}_{solvent\ effect}/RT$ and $\Delta G^{assoc}_{gas}/RT$ versus carbon number for the aliphatic alcohols

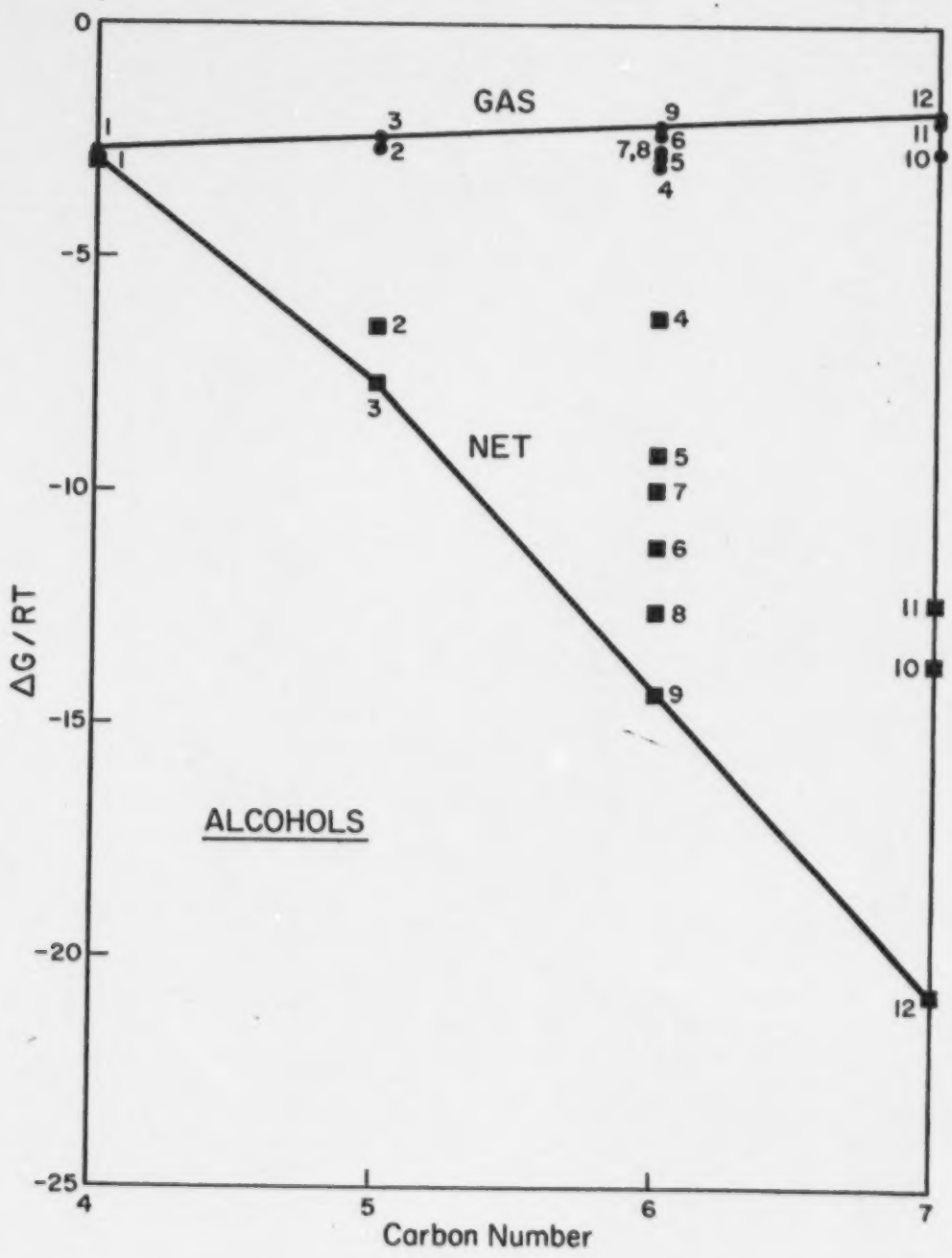

size of the alcohol increases. The gas phase term is fairly constant with carbon number when compared with NET which substanciates earlier assumptions made in the cϕ theory which resulted in neglecting the gas phase contribution. Figure 9 shows GAS and SOLVENT versus carbon number. The lines are again through the linear compounds and diverge with increasing carbon number. The GAS curve increases (becomes less negative) with carbon number which, when compared with Eq. (49), predicts a decrease in adsorption. SOLVENT however decreases with carbon number and when compared with Eq. (8) predicts an increase in adsorption. All of the branched compounds lie above the SOLVENT curve indicating that they adsorb less than their linear counterparts from solution. The reverse is true in the gas phase where all of the branched compounds are below the GAS curve predicting greater adsorption than their linear isomers. This effect is confirmed experimentally.

Eq. (49) is shown as the theoretical line on Figure 10 and the experimental points for the four linear alcohols fall very close to this line. Figure 10 also shows the experimental points for these compounds when adsorbed from the liquid phase. The cϕ theory predicts a linear relationship between $\ell nQ°b$ and SOLVENT. This is shown by the best fit line which correlates the data quite well ($r = 0.979$). Thus the reversal in the order of preferential adsorption due to the presence of water is observed experimentally and substanciated theoretically.

For this reversal to occur, the dominant mechanism for equilibrium adsorption onto activated carbon must be different in the vapor and aqueous phase. Although little quantitative information is known about the surface characteristics of activated carbon and its influence on organic adsorptive selectivity, essentially two types of interactions are thought to dominate. The first can be characterized by van der Waals physical interactions and occurs on a majority of the surface (on basal planes). The second type of surface interaction, which occurs at the more reactive edges of the microcrystallites, can be characterized by attractive polar interactions due to, for example, hydrogen bonding and electrostatic forces. These specific interactions result from the surface heterogeneity and the presence of oxides, hydroxyls, and other groups on the surface.

Figure 6 shows that the adsorption capacities for alcohols are much higher for gas adsorption than liquid phase adsorption. Thus gas adsorption is most likely dominated by van der Waals dispersion interactions. This is confirmed theoretically since the dispersion contribution to the surface free energy, γ_{ℓ}^{d} from Eq. 39), decreases with increasing alcohol size. Smaller molecules will exhibit a larger van der Waals interaction and thus a higher adsorption capacity.

The situation is different when a polar solvent such as water is present. The polar sorbent sites are most likely masked by the highly polar water molecules, so again most adsorption takes place on the non-polar basal planes. In the aqueous phase, however, hydrophobic interactions are important. These

Figure 9. $\Delta G^{assoc}_{gas}/RT$ and $\Delta G^{assoc}_{solvent}/RT$ versus carbon number for the aliphatic alcohols

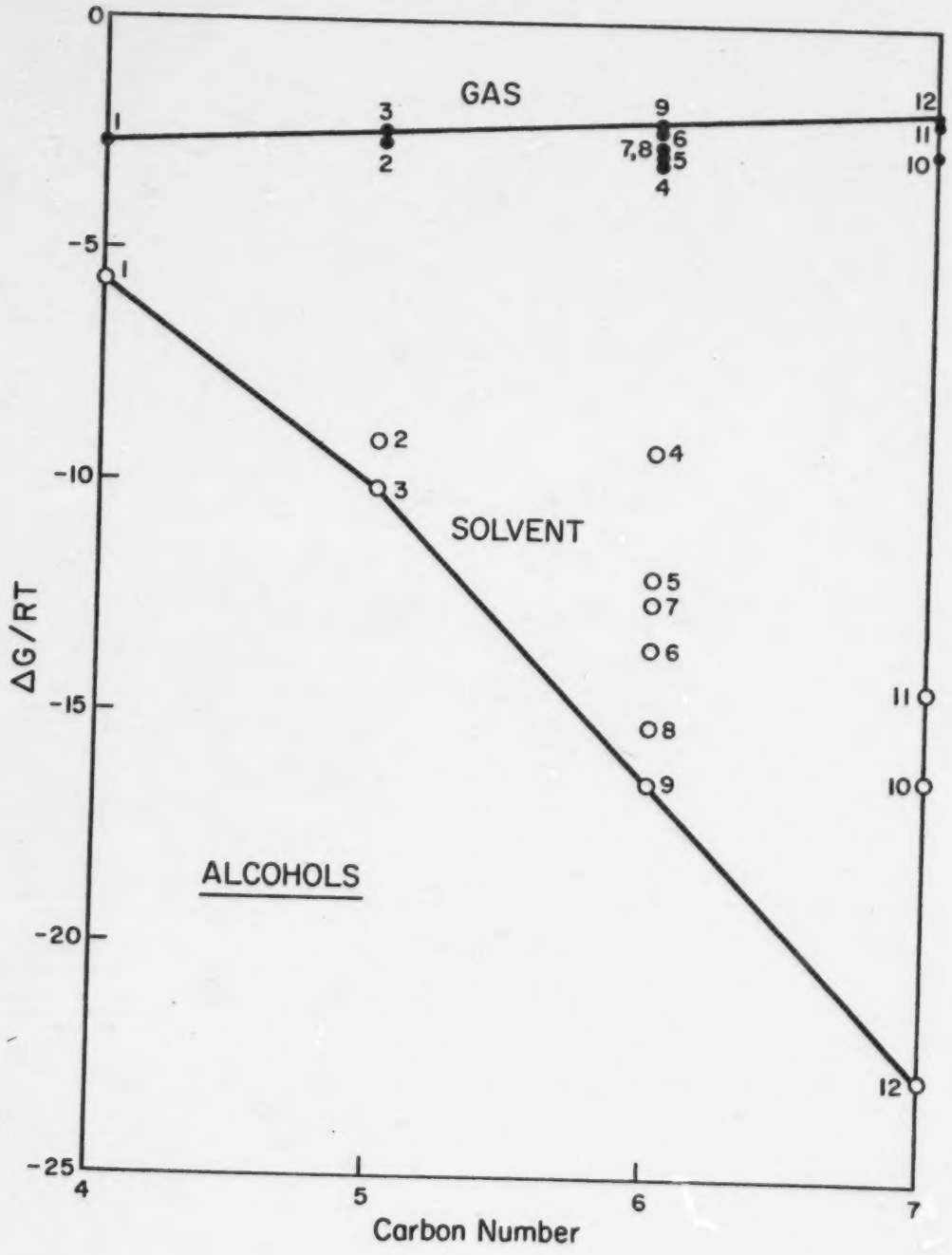

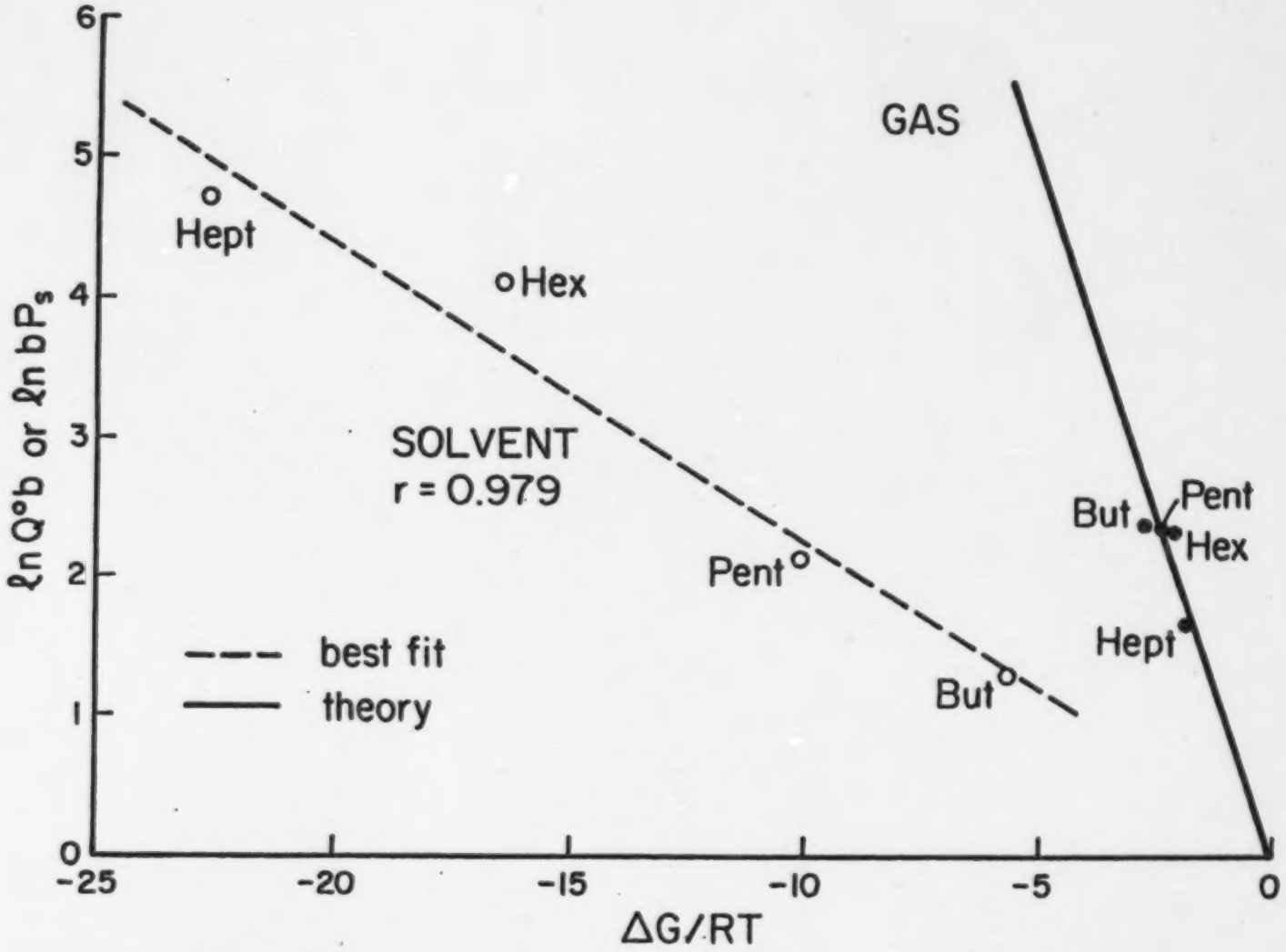

Figure 10. $\ln Q°b$ and $\ln bp_s$ as a function of $\Delta G^{assoc}_{solvent}$ and ΔG^{assoc}_{gas} respectively.

are characterized by ΔG^{net}_{cav}, Eq. (12). Since the hydrophobic interactions increase with increasing alcohol size the reversal in the rank order of adsorption between the vapor and liquid phase is thereby explained.

The gas phase term can be used to calculate $\Delta G^{assoc}_{solvent}$ not only for the alcohols for which experimental gas phase isotherms are available but also for the other components for which experimental isotherms in the aqueous phase only are available. As seen from Table 4, γ^d_s is fairly constant and in fact is a property of the particular activated carbon considered. The value of γ^d_s (319.1 ergs/cm^2) may therefore be used not only for all of the alcohols, but for any compound being adsorbed onto Filtrasorb 400 activated carbon.

The correlation coefficient is r = 0.939 indicating a good linear fit. Figure 11 shows the correlation coefficients of $\ell n\ Q°b$ versus SOLVENT, NET (r = 0.946), TSA (r = 0.926) and MW (r = 0.720). Also shown are the confidence intervals with respect to SOLVENT at various levels of confidence. From Figure 11 we can say with greater than 95% confidence that SOLVENT is a better correlating parameter than MW but we cannot say that TSA or NET give any different correlation than SOLVENT since they are both well within the 50% confidence limits. Any one of these three parameters could be used to correlate adsorption. From a practical viewpoint, TSA is the simplest and most convenient to use.

Surface Tension Effect on Adsorption

Adsorption isotherms were measured in the liquid phase for 4-n-propylphenol in solvents of varying surface tension. The surface tension was changed by adding varying concentrations of ammonium sulfate salt, to increase the solvent surface tension, or methanol to decrease the solvent surface tension. Table 7 gives the solvent surface tension and the best fit Langmuir parameters for each measured isotherm. Figure 12 shows the adsorption isotherms for ammonium sulfate concentrations of 0.0, 0.571, 0.857 and 1.143 molar. An increase in adsorption with concentration takes place in this range of salt concentrations. Figure 13 shows the isotherms for concentrations of 1.143, 1.429 and 1.714 molar. A decrease in adsorption is noted in this range of salt concentrations. Figure 14 shows the adsorption capacity, Q°, and the adsorbability, $\ell n\ Q°b$, as functions of salt concentration and surface tension. In both cases the first four points follow a linear increasing trend as predicted by Eq. (66). The correlation coefficients for the first four points are 0.971 and 0.990 for Q° and $\ell nQ°b$, respectively. The theory therefore fits the data well up to a certain salt concentratin (around 1.143 M). Above this concentration the data show a decrease in adsorption, deviating from the theory. This tendency may be explained by entropic effects. At high salt concentrations, the salt molecules may hinder the movement of the organic toward the carbon surface, or may induce a precipitation. This may also result in incomplete adsorption within the prescribed 24 hour period. The system may not reach complete equilibrium within this time period.

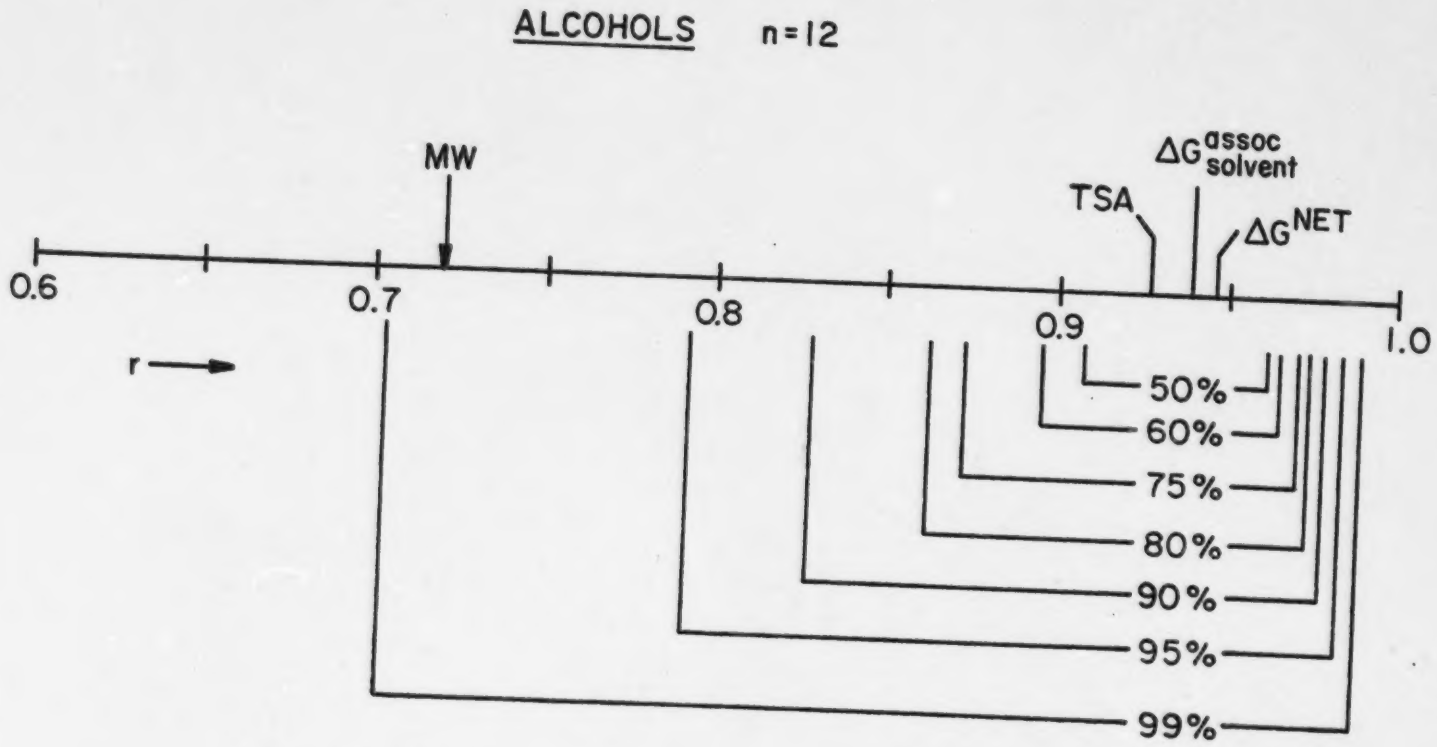

Figure 11. Correlation coefficients and confidence intervals for the correlation of ln0°b with solute parameters for the alcohols

TABLE 7

Adsorption Isotherm Measurements Fitted to the Langmuir Model for 4-n-propylphenol in Solvents of Varying Surface Tension

Concentration		γ (ergs/cm^2)	Γ° (mmole/g)	b (ℓ/mmole)	ℓn Γ°b	r
$(NH_4)_2SO_4$ (mole/ℓ)	0.0	72.0	1.874	135.1	5.534	0.9892
	0.571	73.29	2.522	175.6	6.093	0.9787
	0.857	73.97	2.561	303.8	6.657	0.9484
	1.143	74.67	3.120	347.2	6.988	0.8710
	1.429	75.41	2.083	313.7	6.482	0.9575
	1.714	76.18	1.961	247.0	6.183	0.9275
Methanol (v/v)	10%	56.4	1.879	83.6	5.057	0.9630
	20%	48.3	1.574	74.3	4.762	0.9937
	30%	42.7	1.249	57.4	4.272	0.9857
	40%	37.8	0.959	32.8	3.450	0.9889
	50%	35.0	0.623	42.4	3.274	0.9724

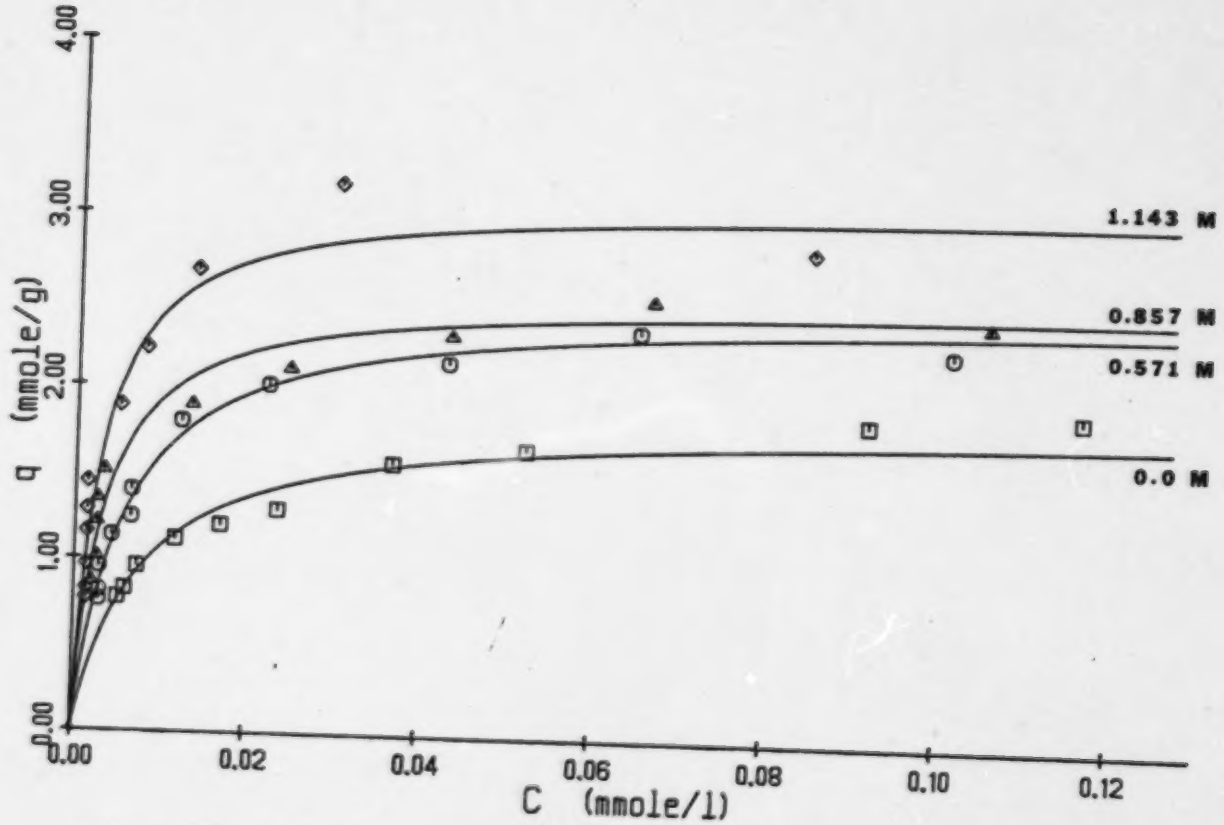

Figure 12. Adsorption isotherms for 4-n-propylphenol in solvents of varying salt concentration (0-1.143 M)

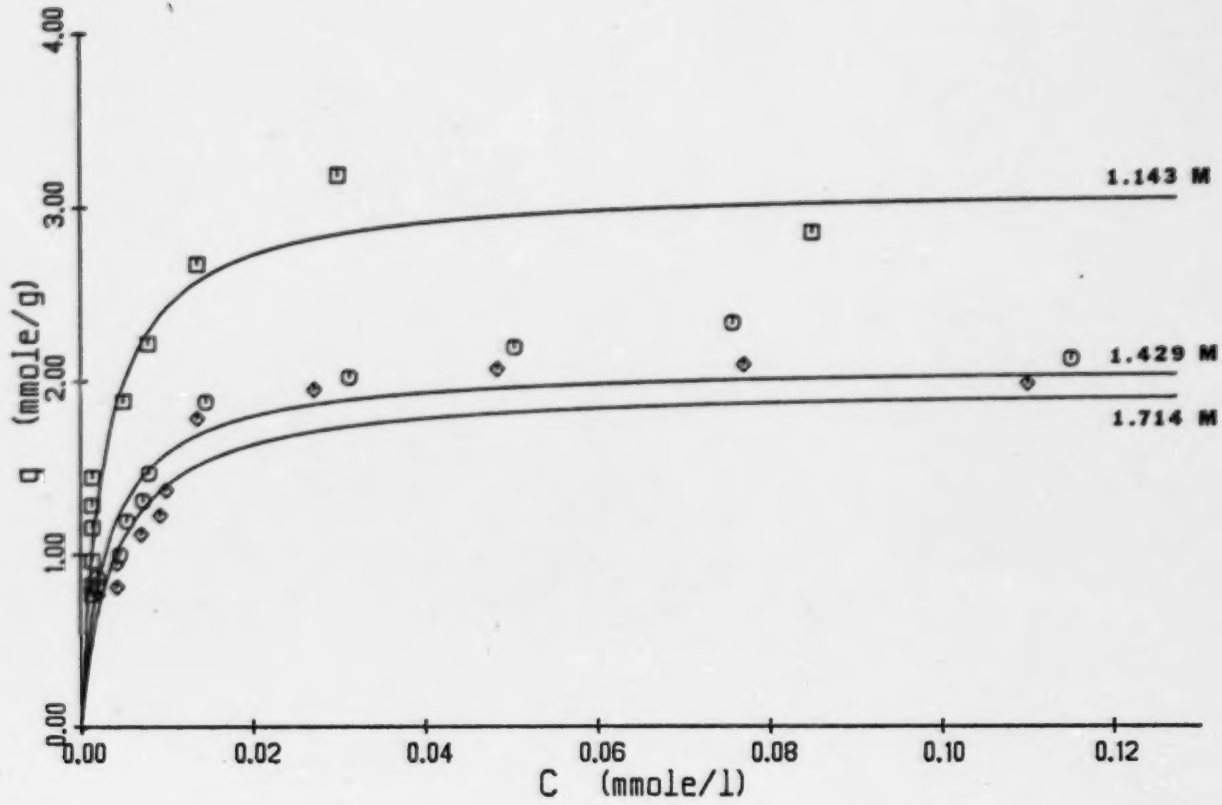

Figure 13. Adsorption isotherms for 4-n-propylphenol in solvents of varying salt concentration (1.143~1.714 M)

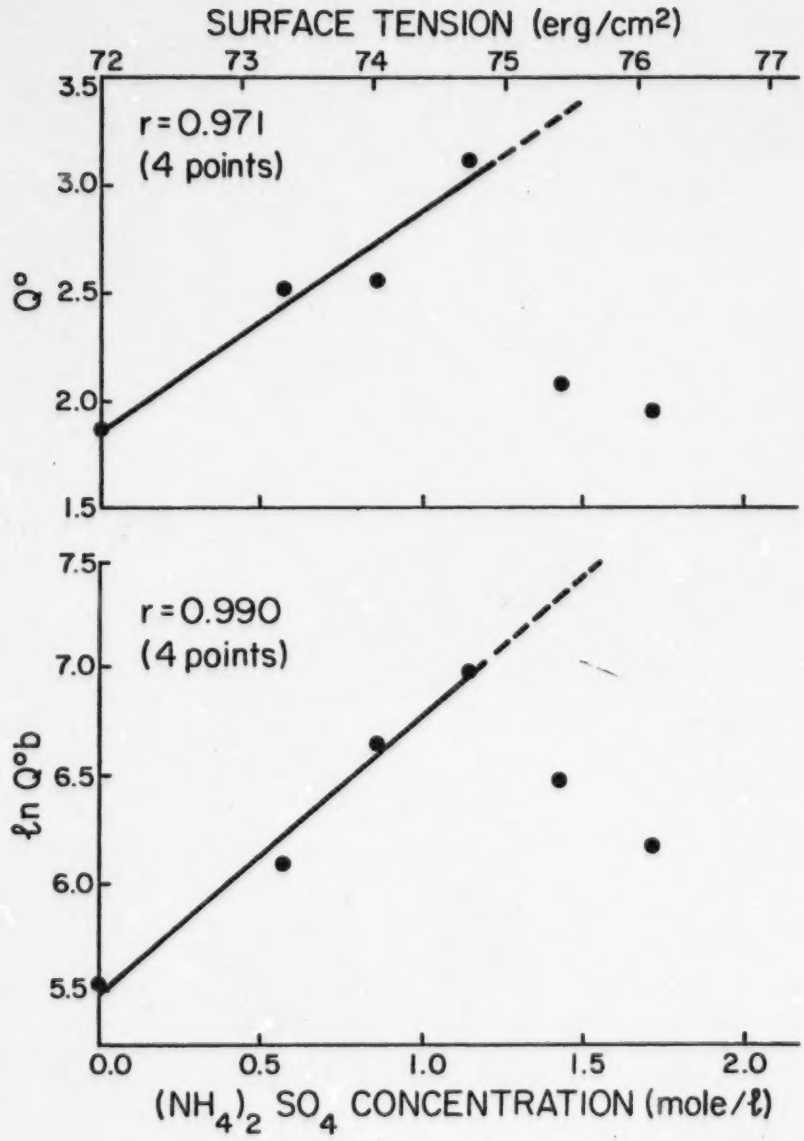

Figure 14. Adsorption capacity and adsorbability versus salt concentration and solvent surface tension for 4-n-propylphenol

Adsorption isotherms with methanol concentrations of 0 - 50 volume percent are shown in Figure 15. A decrease in adsorption with methanol concentration is noticed and also shown on Figure 16 which gives Q° and ℓn Q°b as a function of volume percent methanol. The experimental points seem to fall on straight lines with correlation coefficients of 0.981 and 0.988 for Q° and ℓnQ°b respectively. Since, however, the solvent surface tension is not a linear function of methanol concentration we do not obtain a linear relationship between ℓnQ°b and surface tension as shown in Figure 17. The same type of behavior was found by Horvath et. al. [25] in their work with liquid chromatography. They explained their non-linear data by using an equation similar to Eq. (60). They assumed that the parameter κ^e was not constant but varied with methanol concentration and solved for it for each volume percent of methanol. This method is really only a curve fit however since no satisfactory theory exist at present to calculate a priori the value of κ^e. Another possible explanation for the non-linearity in Figure 17 is a competition effect. Since methanol is a slightly stronger adsorber than water it may displace a significant and increasing amount of water from the carbon surface as the methanol concentration increases. This may in turn make it more difficult for the organic (4-n-propylphenol) to adsorb causing a greater decrease in adsorbability than predicted with decreasing surface tension.

pH Effect on Adsorption

Adsorption isotherms were measured at different pH values (7.00 and 4.75) in the aqueous phase for three linear carboxylic acids on the same activated carbon. All of these isotherms fit the Langmuir form very well. The adsorbability (lnQ°b) versus molecular weight (MW) and total cavity surface area (TSA) of the carboxylic acids are shown in Figs. 18 and 19. Both figures show a large increase in adsorbability due to the lower pH for each acid studied. This can be explained by noting that a low pH increases the relative amount of a-polar undissociated carboxylic acid, and this relatively non-polar species is more easily adsorbed than the dissociated form.

A stronger linear correlation in adsorbability is noted for the neutral pH isotherms as opposed to the low pH isotherms with respect to both molecular weight and TSA. Correlations with adsorbability for the simplified solvophobic theory parameter, TSA in only in good agreement with theoretical prediction at neutral pH. Probably at low pH the active surface groups on the carbon are effected in a complex manner, complicating the correlation.

Multi-Component Adsorption

The relationship between Q_i° and C_i° for the two alkyl phenols are plotted as single solute isotherms in Fig. 20. The analogue Henry's constants, K_i, are calculated from the initial slopes and listed in Table 8.

The experimental single-solute adsorption isotherm data are integrated according to Eq. (68) giving the spreading pressure, π, for each single solute at different values of molar surface area, a. The data sets of π vs. a are

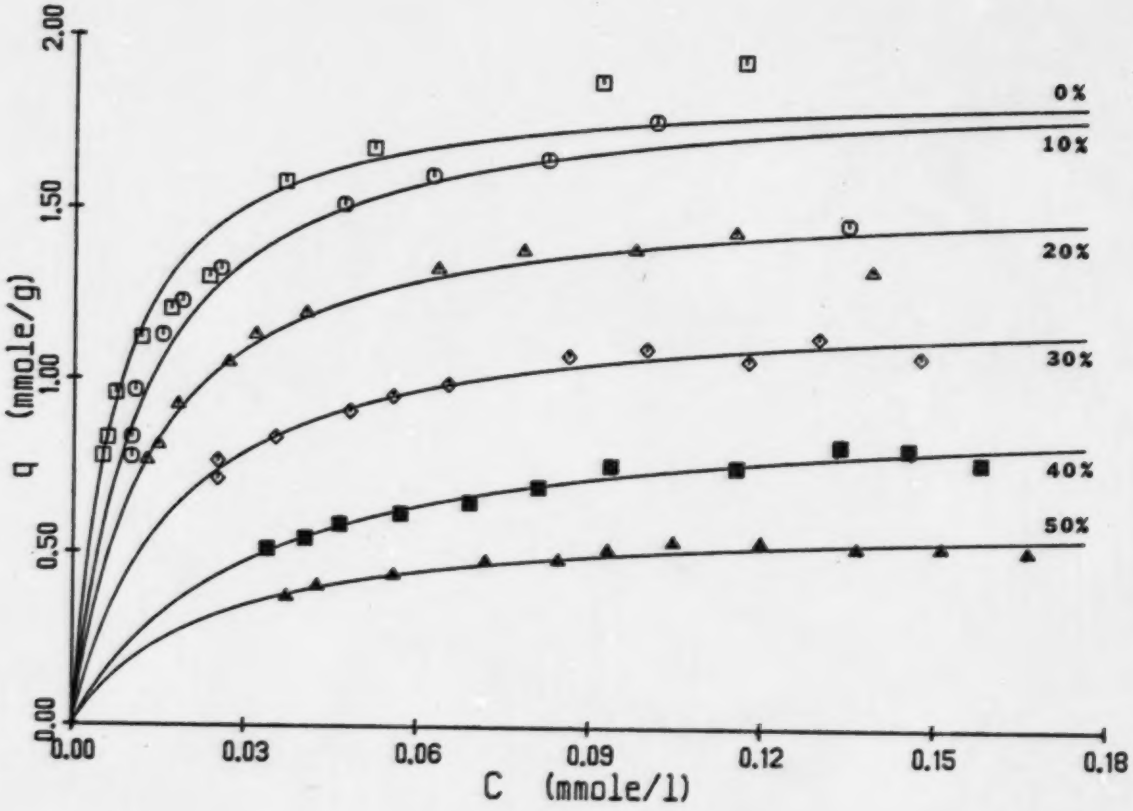

Figure 15. Adsorption isotherms for 4-n-propylphenol in solvents of varying volume percent of methanol

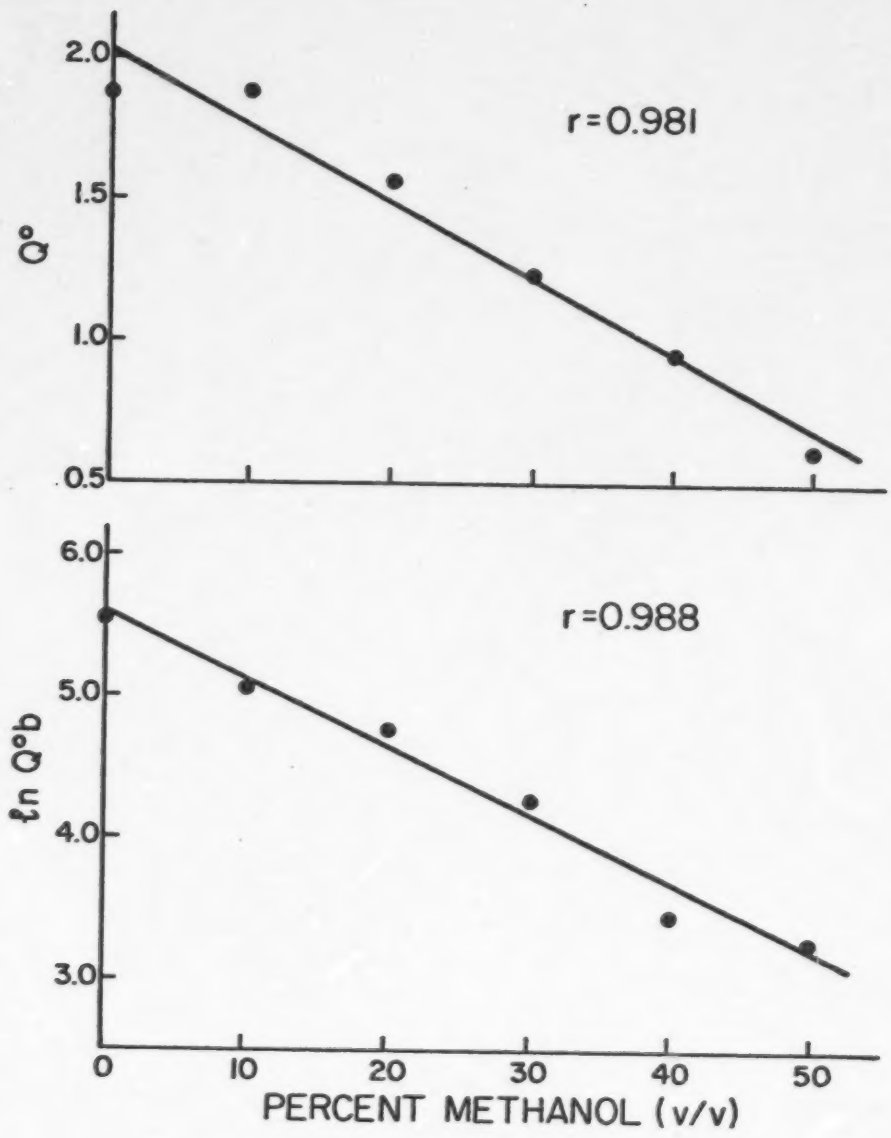

Figure 16. Q° and lnQ°b versus volume percent methanol for 4-n-propylphenol.

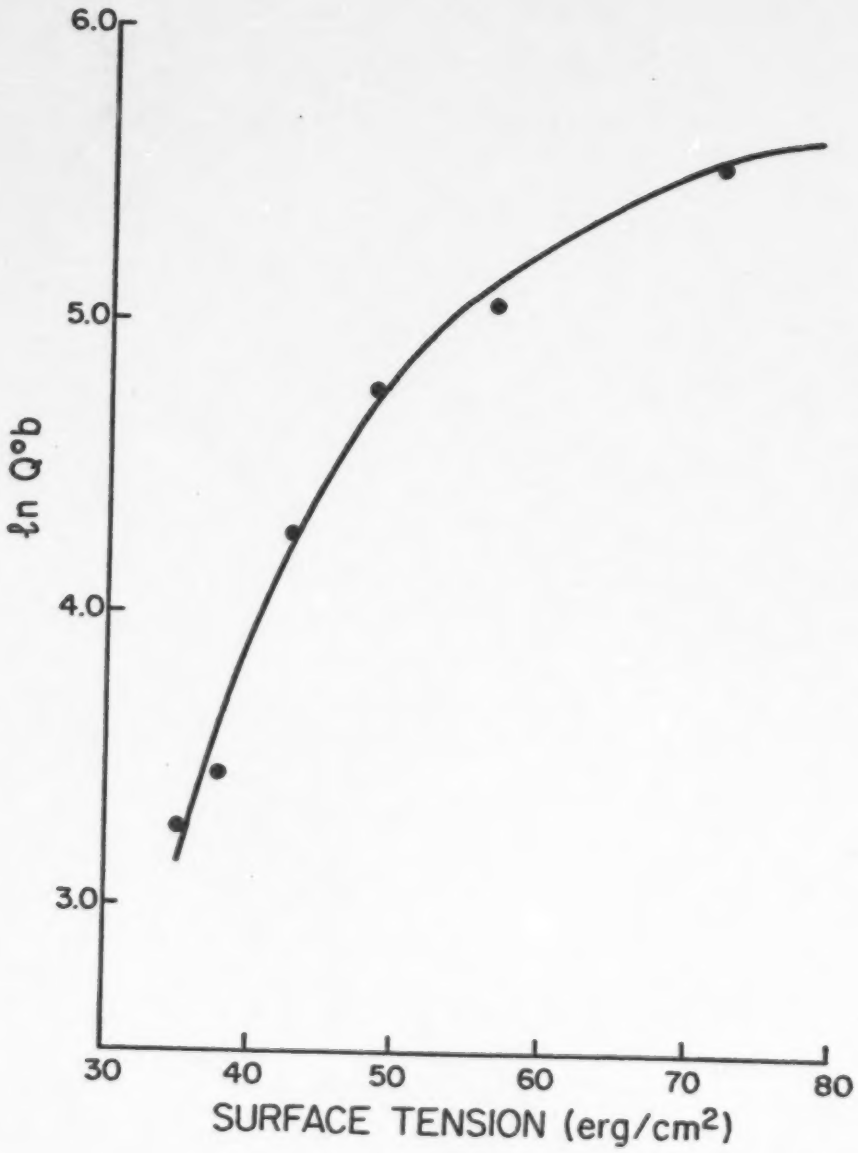

Figure 17. lnQ°b versus solvent surface tension for 4-n-propylphenol.

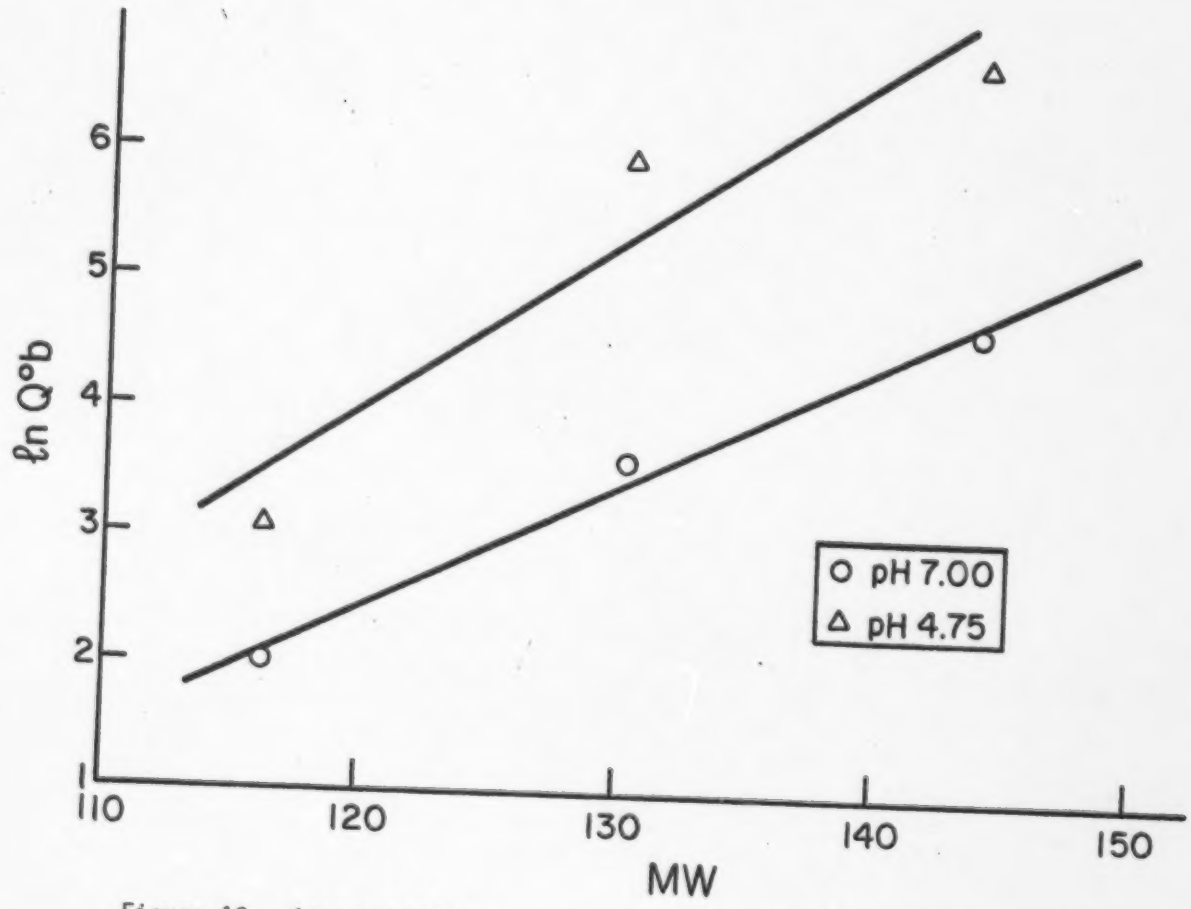

Figure 18. Adsorbability versus molecular weight for carboxylic acids at different pHs

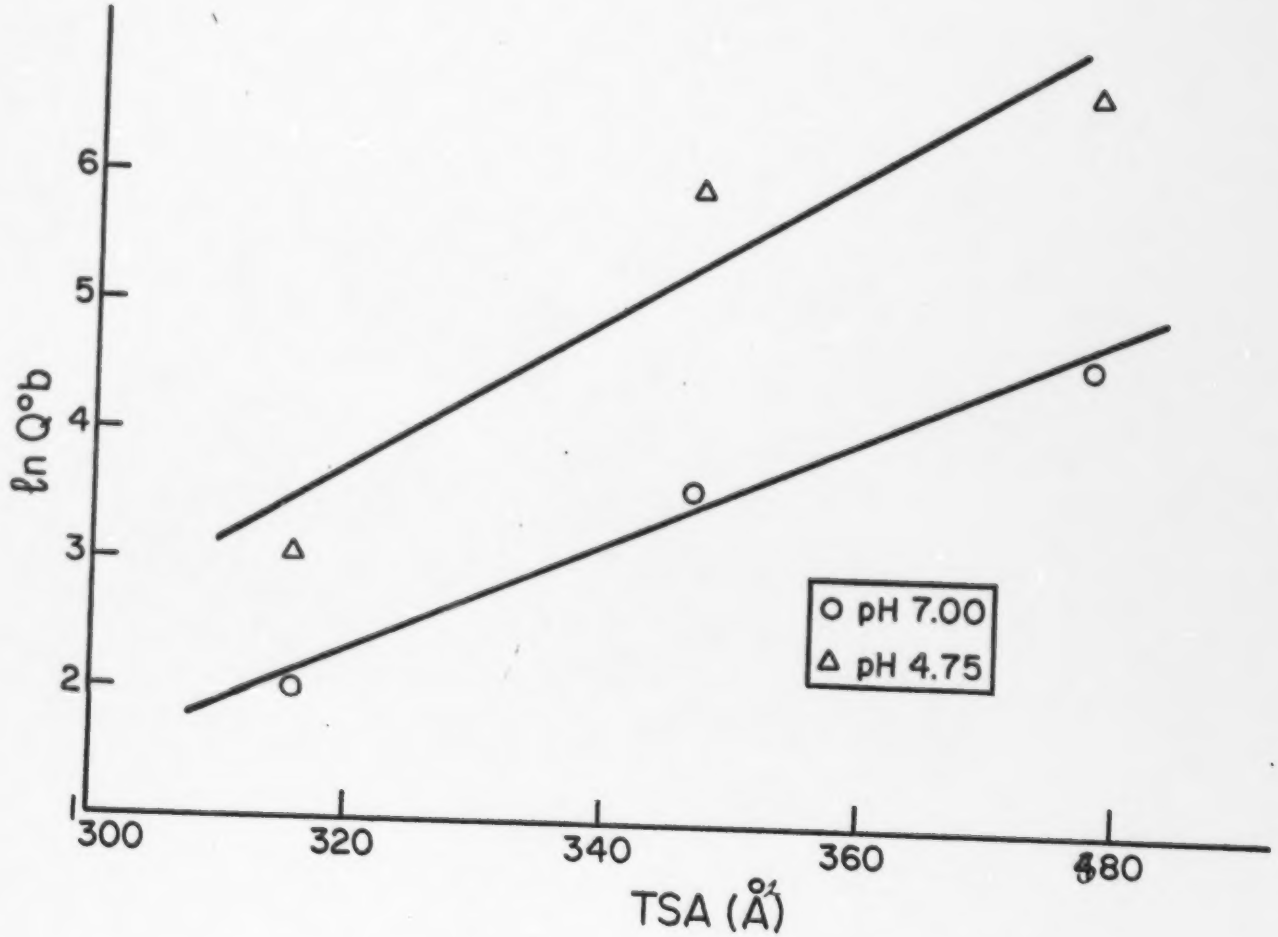

Figure 19. Adsorbability versus total cavity surface area for carboxylic acids at different pH's

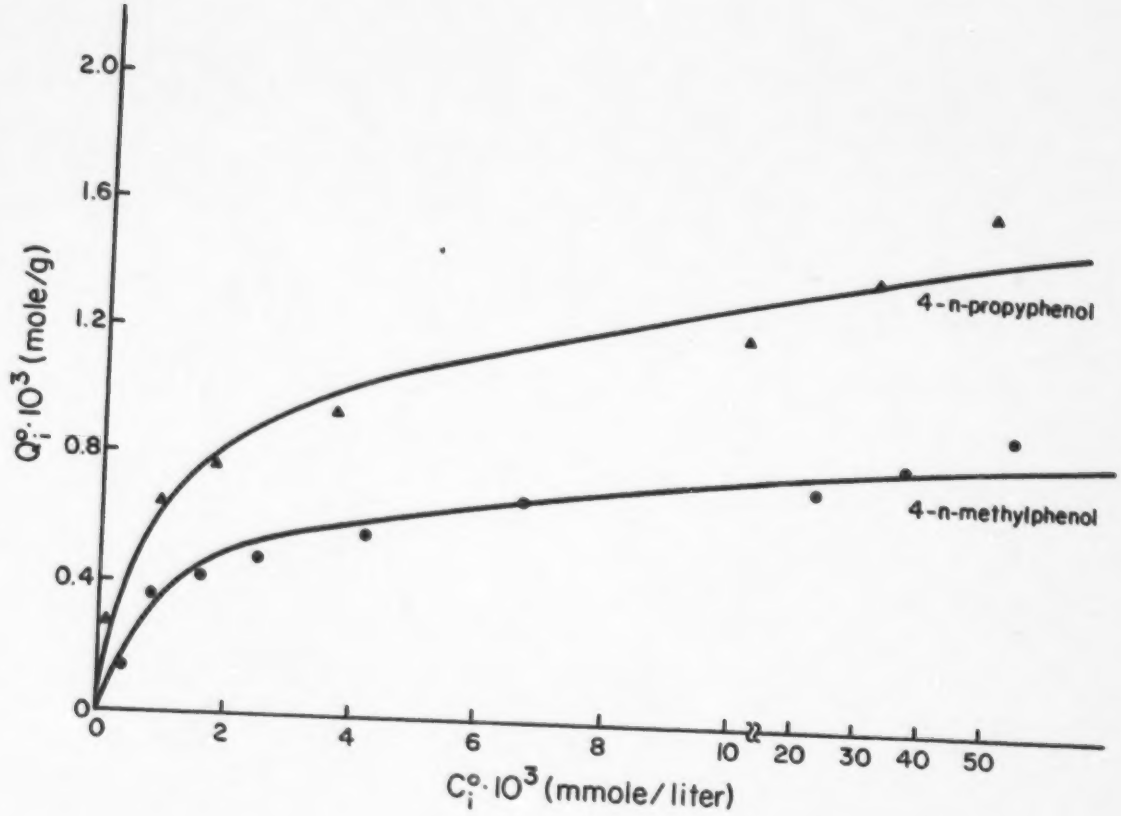

Figure 20. Single-solute adsorption isotherm for alkyl phenols

TABLE 8

Characteristics Constants for Alkyl-Phenols

Solute	α ($J \cdot m^2/mole^2$)	β ($m^2/mole$)	K_i (m)
4-n-propylphenol	1.05×10^9	5.44×10^5	1.066×10^{-3}
4-n-methylphenol	2.00×10^9	1.03×10^6	6.935×10^{-4}

fitted into a 2-dimensional analogue of van der Waals' equation to get the characteristics constants for each solute by curve-fitting. The results are listed and plotted in Table 8 and Fig. 21, respectively. Van der Waals' equation [Eq. (81)] clearly fits the data very well.

The analogue compressibility factor ($\pi a/RT$) can be used as an index to account for non-ideal behavior in the adsorbed phase. Thus, if values of $\pi a/RT$ are larger than 1 non-ideal behavior is suspected. To test if the IAS theory is suitable for the alkyl phenol system, $\pi a/RT$ is plotted against surface loading (Q°_i) and shown in Fig. 22. The assumption of ideal behavior of the adsorbates on the solid surface is only suitable for very low surface loadings, for both single solute adsorption systems. Hence, for an adequate description of the binary alkyl phenol adsorption, the theory should account for non-ideal behavior throughout most of the surface loadings.

Although nineteen experimental mixture points were measured over a three-decade range in concentration and a two-decade range in loading; only one point per calculated line is shown and compared in Radke and Prausnitz's work (6). The reason for this is that it is not possible to control the final solute concentrations. In order to avoid this problem in testing the theory, an iterative scheme using material balances for obtaining the final equilibrium concentrations is developed and shown in Fig. 23.

In Figs. 24 and 25 the experimental binary adsorption data and the predicted results for two different initial concentrations of the alkyl phenols in the mixtures are shown. Solid lines and dotted lines are calculated using the IAS theory and the theory based on the equation of state, respectively. Agreement between predicted and experimental results is good for the latter theory using van der Waals' equation, especially in the higher surface loading region compared to that predicted by the IAS theory. It appears that as Radke and Prausnitz have pointed out (6), the IAS theory is most suitable for quantitative prediction of binary adsorption of small organic molecules with similar adsorption characteristics.

The large deviations between experimental and predicted results by the IAS theory for the weak adsorbate (4-n-methylphenol) can be explained with Equation (67). Since propylphenol is preferentially adsorbed, its mole fraction in the surface phase is close to unity. Thus, the mole fraction of the second component, methylphenol, is very small. Since the loading of methylphenol is calculated from $C^\circ_i = C_i/Z_i$, a very small value of Z_i will give a very large value in C°_i, well beyond the limits of its isotherm. No matter what functional form is used, the extrapolation of an isotherm over a long distance could introduce a significant error.

In Figs. 24 and 25, it can be seen that the predictions using the IAS theory fall above and below the experimental observations for the stronger and weaker adsorber, respectively. These deviations provide a measure of the non-ideality of the binary adsorption system.

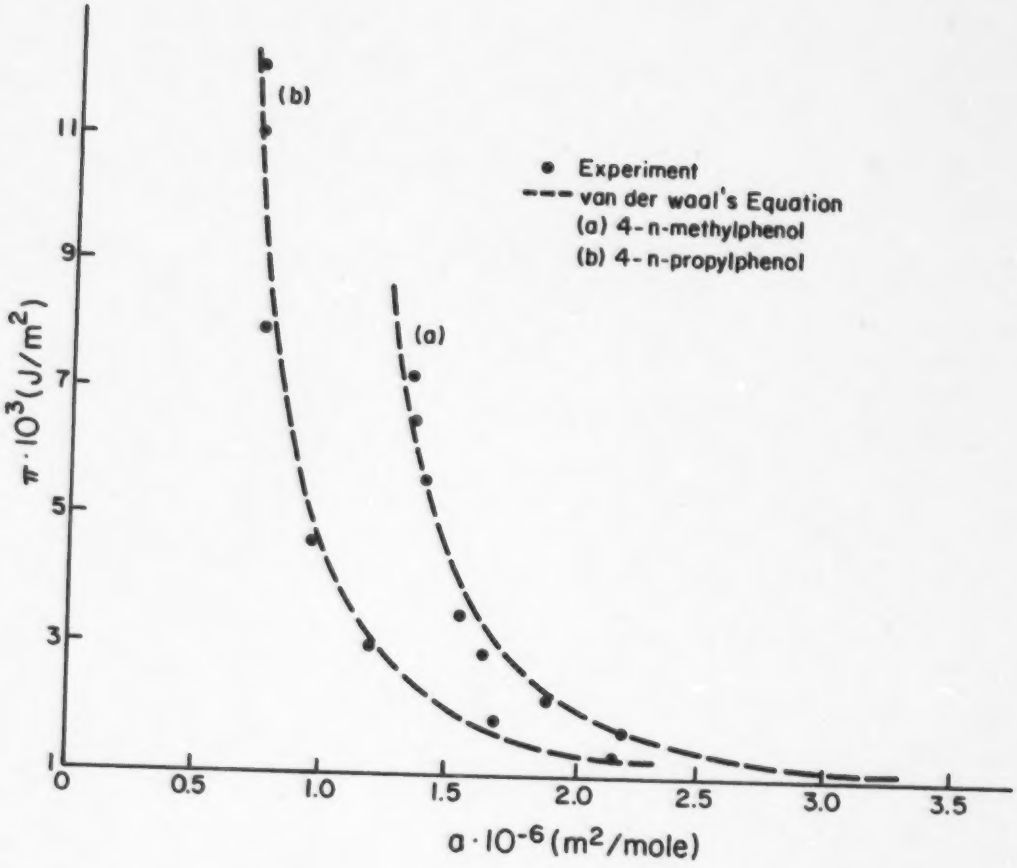

Figure 21. Surface-tension isotherm for alkyl phenols

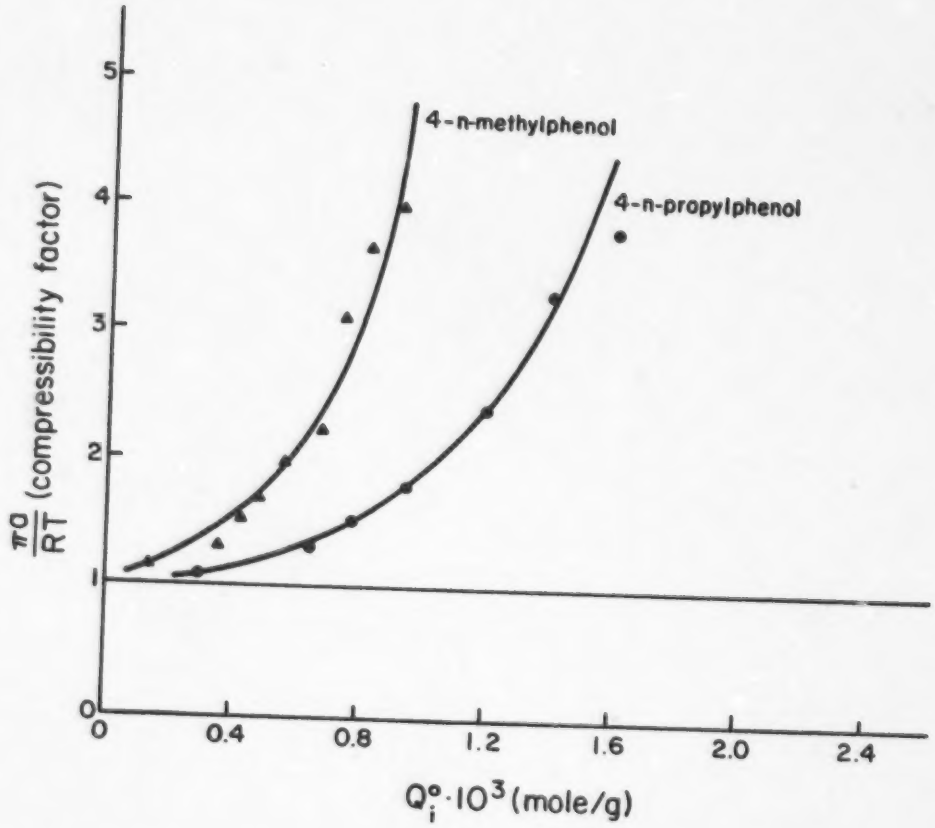

Figure 22. The analog compressibility factor as a function of adsorbed alkyl phenols

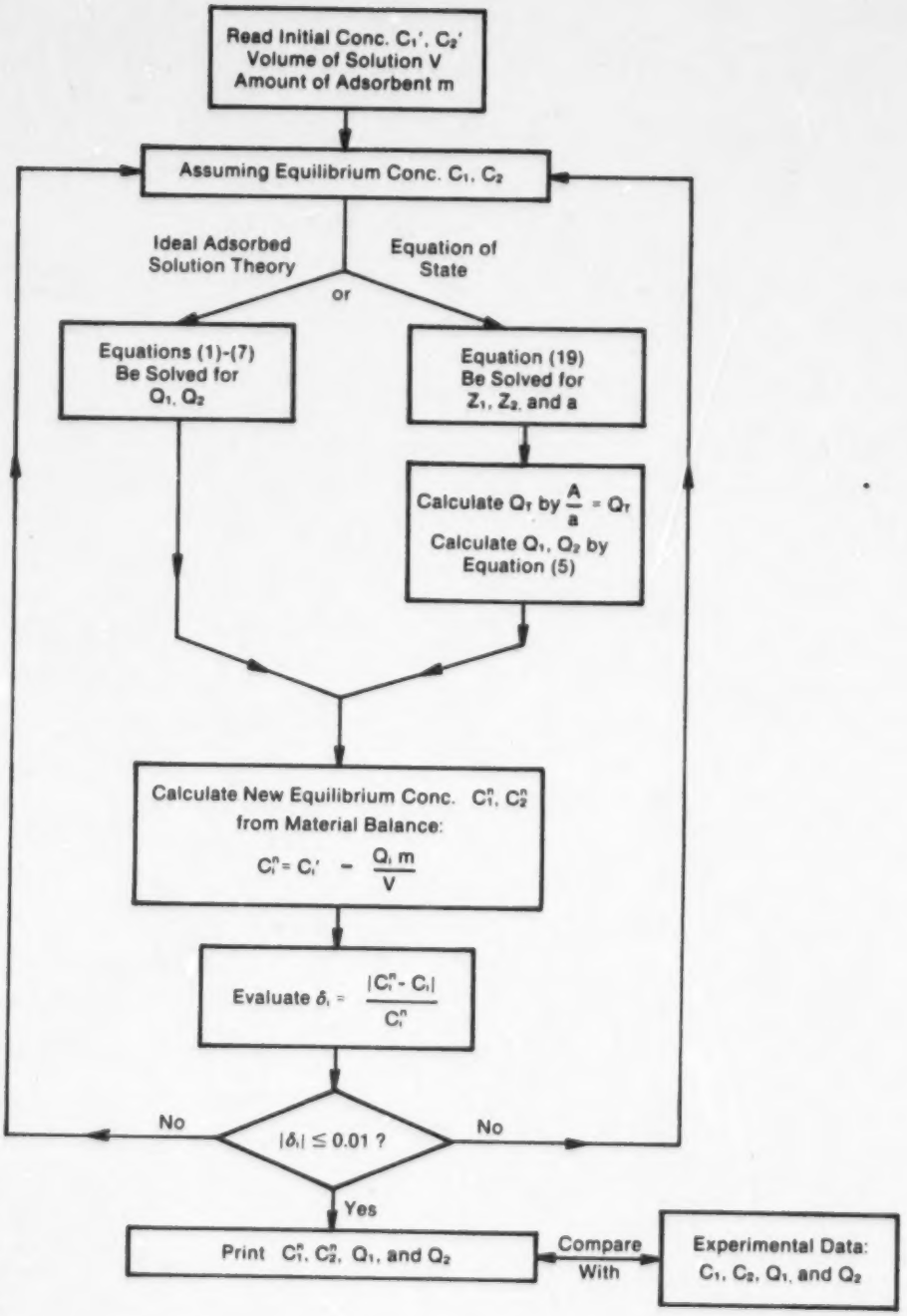
Read Initial Conc. C_1', C_2'
Volume of Solution V
Amount of Adsorbent m
Assuming Equilibrium Conc. C_1, C_2
Ideal Adsorbed Solution Theory
or
Equation of State
Equations (1)-(7) Be Solved for Q_1, Q_2
Equation (19) Be Solved for Z_1, Z_2, and a
Calculate Q_T by $\frac{A}{a} = Q_T$
Calculate Q_1, Q_2 by Equation (5)
Calculate New Equilibrium Conc. C_1^n, C_2^n from Material Balance:
$C_i^n = C_i' - \frac{Q_i m}{V}$
Evaluate $\delta_i = \frac{|C_i^n - C_i|}{C_i^n}$
No
$|\delta_i| \leq 0.01$?
No
Yes
Print C_1^n, C_2^n, Q_1, and Q_2
Compare With
Experimental Data: C_1, C_2, Q_1, and Q_2

Figure 23. The iterative scheme for testing theory

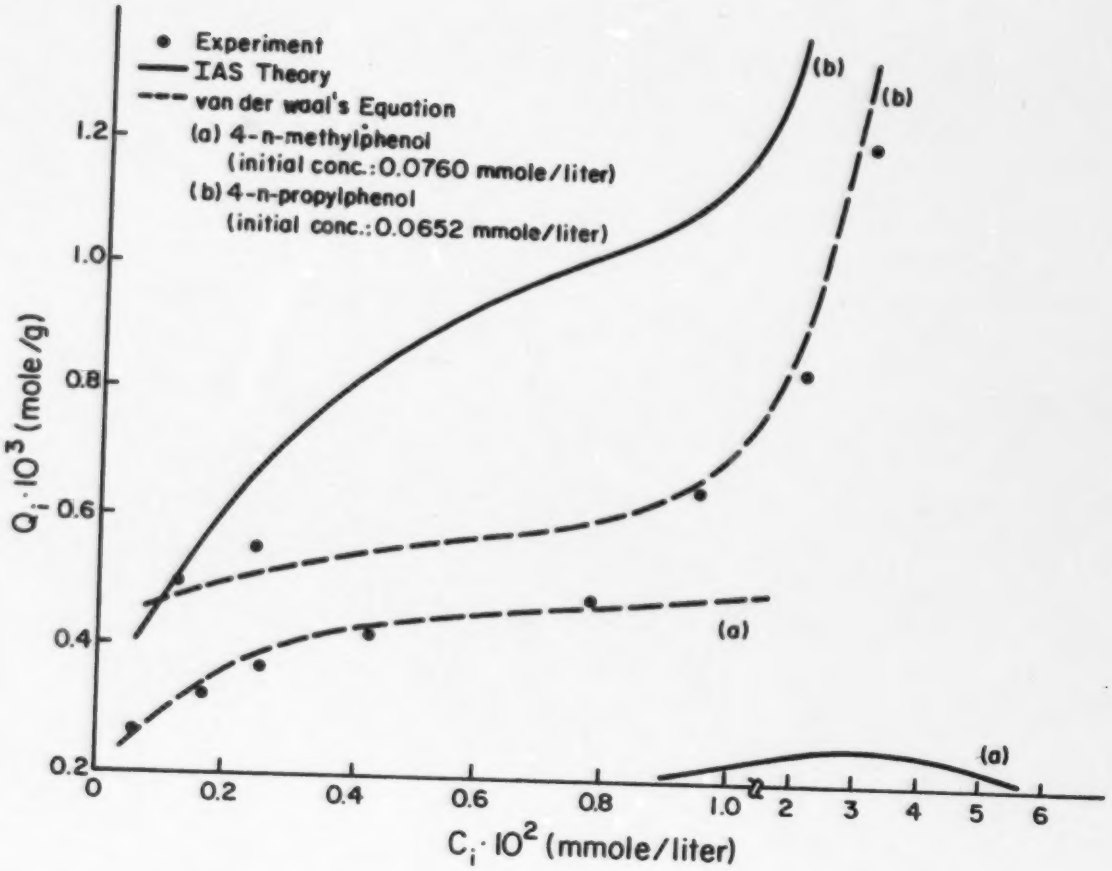

Figure 24. Adsorption from aqueous multi-solute system (4-n-methylphenol and 4-n-propylphenol) at low initial concentrations

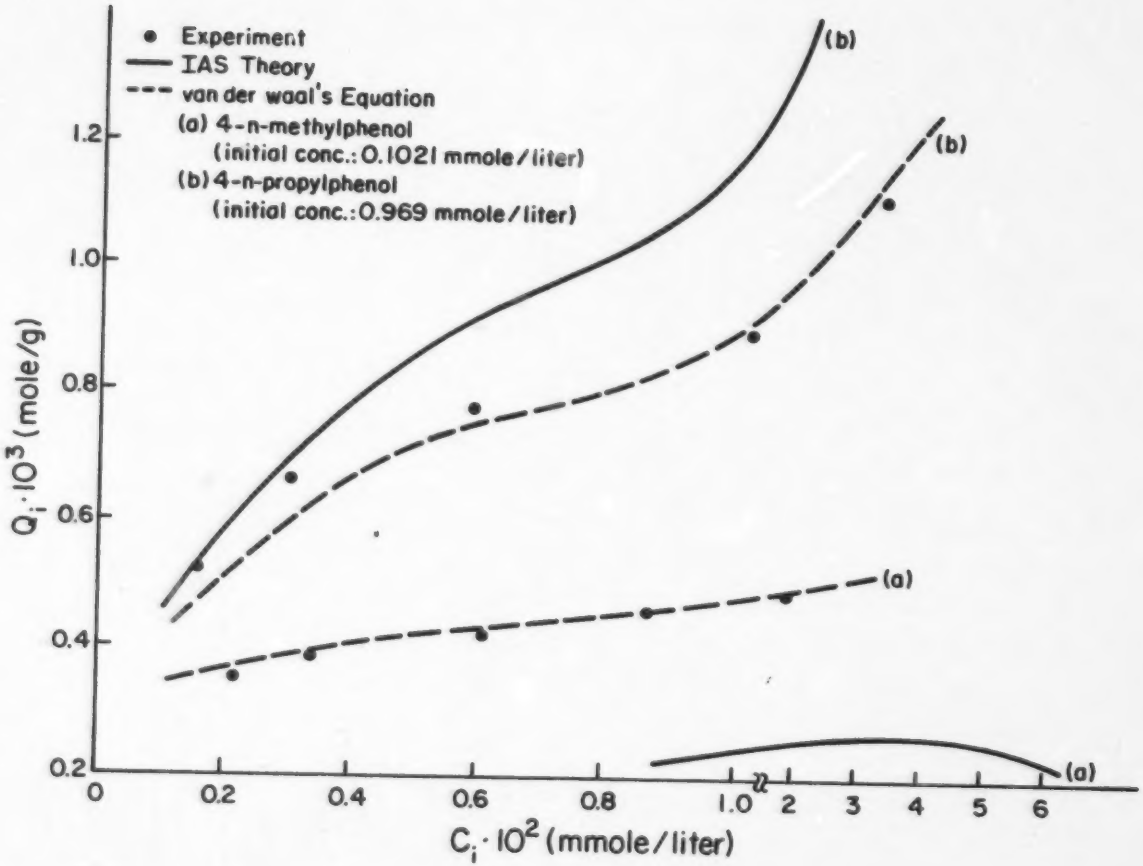

Figure 25. Adsorption from aqueous multi-solute system (4-n-methylphenol and 4-n-propylphenol) at higher initial concentrations

REFERENCES

1. McCreary, J.J. and V.L. Snoeyink, Am. Water Works Assoc. J., 69(8):437-444 (1977).

2. Shuval, H.I., Water Renovation and Reuse, Academic Press, Inc., New York, 1977, pp. 33-72.

3. Preliminary Assessment of Suspected Carcinogens in Drinking Water, Interim Report to Congress, U.S. EPA Office of Toxic Substances, Washington, D.C., 1975.

4. Gibbs, J.W., Scientific Papers, 1, 219, Langman and Green and Co., New York, 1906.

5. Myers, A.L. and J.M. Prausnitz, "Thermodyanmics of Mixed-Gas Adsorption", A.I.Ch.E. Journal, 11, 121 (1965).

6. Radke, C.J. and J.M. Prausnitz, "Thermodynamics of Multi-Solute Adsorption from Dilute Liquid Solutions", A.I.Ch.E. Journal, 18, 761 (1972).

7. Manes, M., "The Polanyi Adsorption Potential Theory and its Applications to Adsorption from Water Solution onto Activated Carbon", "Activated Carbon Adsorption of Organics from Aqueous Phase", V.1, McGuire, M.J. and I.H. Suffet, ed., Ann Arbor Science (1980).

8. Belfort, G., "Similarity of Ideal Adsorbed Solution and Potential Theories for Adsorption from a Bulk Phase onto a Solid Surface", AIChE J., 27, 1021 (1981).

9. McGuire, M.J., I.H. Suffet, "The Calculated Net Adsorption Energy Concept", in "Activated Carbon Adsorption of Organics from the Aqueous Phase", V.1, McGuire, M.J. and I.H. Suffet, ed., Ann Arbor Science Publications, MI (1980).

10. Altshuler, G.L. and G. Belfort, "Selective Adsorption of Organic Homologues onto Activated Carbon from Dilute Aqueous Solutions, Solvophobic Interaction Approach: III. Branching and Predictions", in "Treatment of Water by Granular Activated Carbon", Advances in Chemistry Series No. 202, McGuire, M.J. and I.H. Suffet, ed., Am. Chem. Soc., Washington, D.C., 1983.

11. Belfort, G., Altshuler, G.L., Thallum, K.K., Feerick, C.P., and Woodfield, K.L., "Selective Adsorption of Organic Homologues on Activated Carbon from Dilute Aqueous Solutions. Solvophobic Interaction Approach: IV. Effect of Simple Structural Modifications with Aliphatics", AIChE J., 30, 197 (1984).

12. Belfort, G., Altshuler, G.L., Thallum, K.K., Feerick, C.P., and Woodfield, K.L., "Selective Adsorption of Organic Homologues on Activated Carbon from Dilute Aqueous Solutions. Solvophobic Interaction Approach: V. The Effect of Simple Structural Modifications with Aromatics", to be published in "Fundamentals of Adsorption" (A.L. Myers and G. Belfort, ed.) AIChE Press, New York (1984).

13. Myers, A.L. and S. Sircar, "Theory of Correspondence for Adsorption from Dilute Solutions on Heterogeneous Adsorbents", in "Treatment of Water by Grannular Activated Carbon", Advances in Chemistry Series No. 202, McGuire, M.J. and I.H. Suffet, ed., Am. Chem. Soc., Washington, D.C., 1983.

14. Everett, D.H., "Thermodynamics of Adsorption from Solution", to be published in "Fundamentals of Adsorption", (A.L. Myers and G. Belfort, ed.), AIChE Press, New York (1984).

15. Fowkes, F.M., "Attractive Forces at Interfaces", in "Chemistry and Physics of Interfaces", Sydney Ross, ed., Am. Chem. Soc., Washington, D.C., 1965.

16. Neuhaus, D.M., R.J. Weigand, and G. Belfort, "Difference Between Gas and Liquid Phase Adsorption: Solvophobic Theory and Experiment. VI", submitted for publication (1984).

17. Minka, C. and A.L. Myers, "Adsorption from Ternary Liquid Mixtures on Solids", A.I.Ch.E. Journal, 19, 453 (1973).

18. Wilson, G.M., "Vapor-Liquid Equilibrium: XI. A New Expression for the Excess Free Energy of Mixing", J. Am. Chem. Soc., 86, 127 (1964).

19. Abrams, D.S. and J.M. Prausnitz, "Statistical Thermodynamics of Liquid Mixtures: A New Expression for the Excess Gibbs Energy of Partly and Completely Miscible Systems", AIChE J., 21, 116 (1975).

20. Walpole, R.E. and R.H. Myers, Probability and Statistics for Engineers and Scientists, 2nd ed., MacMillan PUblishing Co., Inc., NY, pp. 280-288 (1978).

21. Documenta Geigy, Scientific Tables, 6th ed., Konrad Diem, ed., J.R. Geigy S.A., Basle, Switzerland.

22. Sinanoglu, O., "Solvent Effects on Molecular Associations", in Molecular Associations in Biology, B. Pullman, ed., Academic Press, N.Y., 427 (1968).

23. Halicioglu, J., and O. Sinanoglu, "Solvent Effects on Cis-Trans Azobenzene Isomerization", Ann. N.Y. Acad. Sci., 158, 308 (1969).

24. Sinanoglu, O., "The Solvophobic Theory for the Prediction of Molecular Conformations and Biopolymer Bindings in Solutions with Recent Direct Experimental Tests", Int. J. Quant. Chem., 18, 381 (1980).

25. Horváth, C., W. Melander, and I. Molnar, "Solvophobic Interactions in Liquid Chromatography with Nonpolar Stationary Phases", J. Chrom., 125, 129 (1976).

26. Melander, W., and C. Horváth, "Salt Effects on Hydrophobic Interactions in Precipitation and Chromatography of Proteins:An Interpretation of the Lyotropic Series", Archives of Biochem. and Biophys., 183, 200 (1977).

27. Horváth, C. and W. Melander, "Reversed-phase Chromatography and the Hydrophobic Effect", Chromatographia, 11, 262 (1978).

28. Horváth, C. and W. Melander, "Thermodynamics of Hydrophobic Adsorption", in Activated Carbon Adsorption of Organics from the Aqueous Phase, ed. I. H. Suffet and M. J. McGuire, pp. 65-89, Ann Arbor Science Publishers, Ann Arbor, (1980).

29. Quayle, O.R., "The Parachors of Organic Compounds", Chem. Rev., 53, 439 (1953).

30. Reid, R.C., J.M. Prausnitz, T.K. Sherwood, The Properties of Gases and Liquids, 3rd ed., McGraw-Hill, NY, 602 (1977).

31. Innes, W.B. and H.H Rowley, J. Phys. Chem., 46, 548 (1942).

32. Ross, S. and J.P. Olivier, On Physical Adsorption, Interscience, 1964.

33. Van Ness, H.C., "Adsorption of Gases on Solids", Ind. Eng. Chem. Fund., 8, 464 (1969).

34. Hoory, S.E. and Prausnitz, J.M., "Monolayer Adsorption of Gas Mixtures on Homogeneous and Heterogeneous Solids", Chem. Eng. Sci. 22, 1025 (1967).

35. Smith, G. of Merk, Sharp and Dohm, New Jersey, loaned us a copy of the molecular-build program, designated by MSD.

36. Manufacturing Chemists Association Research Project, Chemical Thermodynamics Properties Center, "Selected Values of Properties of Chemical Compounds", Texas A&M University, College Station, TX (1966).

37. Feerick, C.P., M.E. Thesis, Department of Chemical Engineering and Environmental Engineering, Rensselaer Polytechnic Institute, Troy, NY (1981).

38. Weast, R.C., ed., Handbook of Chemistry and Physics, CRC Press, Boca Raton, Florida (1983).